The *Arabidopsis SUD1* Gene, encoding a putative E3 Ubiquitin Ligase, is a Positive Regulator of the 3-Hydroxy-3-Methylglutaryl Coenzyme A Reductase Activity

Running Title: SUD1 in the regulation of HMGR activity

Verónica G. Doblas,[a,1] Vítor Amorim-Silva,[b,1] David Posé,[a] Abel Rosado,[a] Alicia Esteban,[a] Montserrat Arró,[c] Herlander Azevedo,[b] Aureliano Bombarely,[a] Omar Borsani,[d] Victoriano Valpuesta,[a] Albert Ferrer,[c] Rui M. Tavares,[b] and Miguel A. Botella[a,2]

[a]Instituto de Hortofruticultura Subtropical y Mediterránea, Universidad de Málaga-Consejo Superior de Investigaciones Científicas (IHSM-UMA-CSIC), Departamento de Biología Molecular y Bioquímica, Facultad de Ciencias, Universidad de Málaga, Málaga, Spain

[b]Center for Biodiversity, Functional & Integrative Genomics (BioFIG), Plant Functional Biology Center, University of Minho, Campus de Gualtar, 4710-057 Braga, Portugal.

[c]Department of Molecular Genetics, Centre for Research in Agricultural Genomics (CRAG) (CSIC-IRTA-UAB-UB), Campus UAB, Bellaterra-Cerdanyola del Vallés (Barcelona), and Department of Biochemistry and Molecular Biology, Faculty of Pharmacy, University of Barcelona, Spain.

[d]Laboratorio de Bioquímica, Departamento de Biología Vegetal, Facultad de Agronomía, Universidad de la República, Montevideo, Uruguay (O.B.)

[1]These authors contributed equally to this work. [2] Address correspondence to mabotella@uma.es. The author responsible for distribution of materials integral to the findings presented in this article in accordance with the policy described in the Instructions for Authors (www.plantcell.org) is: Miguel A. Botella (mabotella@uma.es).

14 estimated pages using page calculator

SYNOPSIS

In contrast to animals, little is known in plants about the regulation of HMGR, the rate-limiting enzyme of isoprenoid biosynthesis. Through the identification of second-site suppressors of the *Arabidopsis dry2/sqe1-5* mutant we have identified the putative E3 ubiquitin ligase SUD1 as a novel regulator of HMGR activity. SUD1 is homologous to the yeast Doa10 protein involved in ERAD.

ABSTRACT

The 3-hydroxy-3-methylglutaryl-CoA reductase (HMGR) enzyme catalyzes the major rate-limiting step of the mevalonic acid (MVA) pathway from which sterols and other isoprenoids are synthesized. In contrast to the extensive knowledge on the regulation of HMGR in yeast and animals, little is known in plants. In order to identify new regulatory components of the MVA pathway in plants we have performed a genetic screen for second-site suppressor mutations of the *Arabidopsis dry2* mutant that show decreased squalene epoxidase activity. We show that mutations in *SUD1* recover most developmental defects in *dry2* through changes in HMGR activity. *SUD1* encodes a putative E3 ubiquitin ligase that shows sequence and structural similarity to yeast Doa10 and human TEB4, components of the Endoplasmic Reticulum-Associated Degradation-C (ERAD-C) pathway. While in yeast and animals the alternative ERAD-L/ERAD-M pathway regulates HMGR activity by controlling the protein stability, SUD1 regulates HMGR activity without apparent changes in protein content. These results highlight similarities but also important mechanistic differences among the components involved in HMGR regulation in plants, yeast, and animals.

INTRODUCTION

For sessile organisms such as plants, metabolic plasticity is essential in order to survive in their changing environments (Nicotra et al., 2010). A good example of this plasticity is the thousands of isoprenoid compounds and derivatives that higher plants synthesize from the five-carbon building units isopentenyl diphosphate (IPP) and its isomer dimethylallyl diphosphate (DMAPP) (Bouvier et al., 2005). Plants synthesize IPP and DMAPP by two independent pathways: the mevalonic acid (MVA) pathway, which produces cytosolic IPP (McGarvey and Croteau, 1995; Newman and Chappell, 1999), and the methylerythritol phosphate (MEP) pathway, which is localized in the plastids (Eisenreich et al., 2001; Rodriguez-Concepcion and Boronat, 2002). In higher plants, isoprenoids carry out numerous essential roles in developmental processes including respiration, photosynthesis, growth and reproduction, as well as adaptation to environmental challenges and involvement in plant defense mechanisms against different types of organisms (Tholl and Lee, 2011; Hemmerlin et al., 2012).

The main MVA-derived isoprenoid end products in plants are sterols, which are integral components of the membrane and are essential for plant growth and developmental processes. Other important MVA products are the steroid hormones brassinosteroids, dolichols, that are involved in protein glycosylation, and the prenyl groups used for protein prenylation and cytokinin biosynthesis (Benveniste, 2004; Phillips et al., 2006; Schaller, 2010). A number of studies over the years have shown the importance of a correct sterol composition in plants because of their roles in embryonic pattern formation (Jang et al., 2000), cell division, elongation and polarity (Schrick et al., 2000; Willemsen et al., 2003; Men et al., 2008), vascular patterning (Carland et al., 2010), cellulose accumulation (Schrick et al., 2004), and Reactive Oxygen Species (ROS) production (Posé et al., 2009), and normal miRNA function (Brodersen et al., 2012). Still, little is known about the mechanisms and downstream targets by which isoprenoids in general, and sterols in particular, influence these processes (Boutté and Grebe, 2009; Clouse, 2002).

The 3-hydroxy-3-methylglutaryl-CoA reductase (HMGR) is considered the major rate-limiting enzyme controlling the metabolic flux in early steps of the

MVA pathway (Hemmerlin et al., 2012). The genome of *Arabidopsis thaliana* contains two differentially expressed HMGR genes, *AtHMG1* and *AtHMG2*, (Enjuto et al., 1994) encoding three HMGR isoforms: HMGR1S (short isoform), HMGR1L (long isoform) and HMGR2. HMGR1S and HMGR1L are both encoded by the *AtHMGR1* gene and are identical in sequence, except by an N-terminal extension of 50 amino acid residues in HMGR1L (Lumbreras et al., 1995). HMGR1S has been proposed to have a housekeeping role, whereas HMGR1L and HMGR2 have a more specialized function, which might be required in particular cell types or at specific developmental stages (Suzuki et al., 2004; Suzuki et al., 2009). All plant HMGR variants are targeted to the endoplasmic reticulum (ER) and have the same topology in the membrane (Campos and Boronat, 1995). The diverged N-terminal region and the conserved catalytic domain are located in the cytosol, whereas only a short stretch of amino acids connecting the two transmembrane segments is in the ER lumen. Plant HMGR is modulated by a variety of developmental and environmental signals, and it has been proposed that the major changes in HMGR activity are determined at the transcriptional level whereas the post-transcriptional control allows a finer and faster adjustment (Hemmerlin et al., 2012). In fact, evidence of posttranslational regulation of HMGR has been obtained in *Arabidopsis* plants with enhanced or depleted flux through the sterol biosynthetic pathway (Nieto et al., 2009). Similarly, inhibition of squalene epoxidase (SQE) activity in tobacco BY-2 cells using terbinafine also triggers an increase in HMGR activity, even though it does not induce changes in the HMGR transcript levels (Wentzinger et al., 2002). Mechanistically, a protein phosphatase 2A (PP2A) has been recently identified as a negative regulator of *Arabidopsis* HMGR activity and protein levels (Leivar et al., 2011), still, proteins involved in the post-transcriptional regulation of plant HMGR are mostly uncharacterized.

In plants, SQEs catalyze the conversion of squalene, the first committed precursor of essential MVA-derived isoprenoids, to 2,3-oxidosqualene (Rasbery et al., 2007; Posé et al., 2009; Schaller, 2010). The *Arabidopsis dry2*/*sqe1-5* mutant was identified by its extreme hypersensitivity to drought stress, altered stomatal responses, and root defects. Chemical analysis indicated that the *dry2/sqe1-5* mutant has altered sterol composition in roots but wild-type sterol

composition in shoots, indicating an essential role for SQE1 in root sterol biosynthesis. Importantly, the stomatal and root defects of the *dry2/sqe1-5* mutant are associated with altered production of ROS, establishing a previously unknown link between the MVA pathway and ROS (Posé et al., 2009).

The *dry2/sqe1-5* allele contains a point mutation in the 4th exon that produces a substitution of a conserved glycine by an arginine, resulting in reduced epoxidase activity (Pose et al., 2009). In contrast to the null alleles of *SQE1* that are sterile, *dry2/sqe1-5* plants are fertile, and this characteristic enables its use for genetic analyses. In this work, we used the hypomorphic *dry2/sqe1-5* mutant allele to perform a genetic screen for second-site suppressor mutations in order to identify new genetic components regulating the MVA pathway. Several mutants (named *sud* for *suppressors of dry2 defects*) that reversed most of the *dry2/sqe1-5* developmental phenotypes were isolated. As a result, we identify a previously uncharacterized regulatory element, SUD1, which encodes a protein with sequence and structural homology to the E3 ubiquitin ligases Doa10 in yeast and TEB4 in humans, proteins that are involved in Endoplasmic Reticulum Protein Degradation (ERAD) pathway. Our results indicate that SUD1 functions as a positive post-transcriptional regulator of HMGR activity in *Arabidopsis*.

RESULTS

Phenotypic characterization of the *dry2* suppressors

To identify novel elements controlling the isoprenoid biosynthetic pathway we performed a suppressor screening based on the recovery of the extreme drought hypersensitive phenotype of the previously characterized *dry2* mutant affected in the Squalene Epoxidase 1 (Posé et al., 2009, Supplemental Figure 1). As a result, four independent mutants were selected and named *sud* for *suppressor of dry2* defects, which maintained the reversion of the *dry2* drought hypersensitive phenotype across multiple generations. Identification of the gene affected in the 4 suppressors indicated that the mutations were allelic (see below), and the mutants were subsequently designated *dry2/sud1-1* to *dry2/sud1-4.*

The recovery of the multiple *dry2* phenotypic defects was further analyzed using the *dry2/sud1-1* and *dry2/sud1-2* alleles. The *dry2/sud1-1* and *dry2/sud1-2* mutants showed a restoration of the leaves size and color observed in *dry2* and rendered shoots undistinguishable from those of WT (Figure 1A). This phenotypic recovery of the shoots in the suppressors correlated with the reestablishment of H_2O_2 and O_2^- accumulation to WT levels (Figure 1B). Since the identification of the suppressors was based on the restoration of the *dry2* extreme drought hypersensitivity, we expected that the defective ABA stomatal responses observed in *dry2* would be also restored in the suppressors. As shown in Figure 1C, exogenous application of 20 μM ABA only caused a ~20% reduction in the *dry2* stomatal conductance compared to the ~80% reduction that occurred in WT, *dry2/sud1-1* and *dry2/sud1-2* plants. In addition, the proline content in *dry2/sud1-1* and *dry2/sud1-2* was more similar to WT plants (Figure 1D). These results confirm that the recovery of the *dry2* shoot phenotypes was associated with a restoration of the water relations in the suppressors.

The primary root length of the *dry2/sud1-1* and *dry2/sud1-2* alleles was double than that of *dry2*, reaching ~70% of the WT seedlings (Figure 2A and 2B). *dry2/sud1-1* and *dry2/sud1-2* also exhibited decreased number of lateral roots when compared to *dry2* (Figures 2A and 2C). The striking defects in root

hair length and morphology observed in *dry2* (Posé et al., 2009) were also substantially restored in the suppressors (Figures 2D and 2E). Consistent with the rescue of the root hair growth defects, *dry2/sud1-1* and *dry2/sud1-2* showed WT ROS production at the bulge of the root hair tip (Figure 2F), in contrast with the aberrant *dry2* ROS production caused by an ectopic localization of the NADPH oxidase C (AtrbohC) (Posé et al., 2009).

All four *dry2* suppressors harbor mutations in the *SUD1* gene

As a first step to determine the gene(s) affected by the *sud* mutations we crossed *dry2/sud1-1* and *dry2/sud1-2* and performed an allelism test. As shown in Figure 3A, reciprocal crosses rendered progenies with WT phenotypes suggesting that the *sud1-1* and *sud1-2* mutations were allelic. However, F1 plants from the backcross between the suppressors and *dry2* showed an intermediate phenotype indicating that the mutations were semidominant (Figure 3A and 3B). Based on these results we could not directly infer whether the *sud1-1* and *sud1-2* mutations were allelic (Koornneef et al., 2006).

Next, we used a combination of map-based-cloning and high throughput sequencing to identify the *sud1-1* mutation. For that purpose, the *dry2* mutant allele (L*er* ecotype) was crossed over seven generations into Col-0 to create an introgression line harboring the *dry2* mutation in Col-0 background (*dry2*$^{Col-0}$). Molecular markers demonstrated that *dry2*$^{Col-0}$ was a near isogenic Col-0 line with the *dry2* mutation and this line displayed similar phenotypes as the original *dry2* mutant (Supplemental Figure 2A-2C). Since the *dry2*$^{Col-0}$ line was a suitable parental line for map based cloning, a F_2 population from the cross between *dry2/sud1-1* and *dry2*$^{Col-0}$ was generated. Fine-scale map-based-cloning delimitated the region harboring the *sud1-1* mutation in chromosome IV between the *AT4G33970* and *AT4G34250* loci (Supplemental Figure 2D). High throughput sequencing and analysis of the region containing *sud1-1* determined that the second-site mutation responsible for the *dry2/sud1-1* suppression phenotype was a G-to-A substitution at nucleotide 652 relative to the ATG of the *AT4G34100* gene (hereafter named *SUD1*). This nucleotide change caused a G218R substitution in the predicted SUD1 amino acid sequence (Figure 3C and Supplemental Figure 2D). Rough mapping of the other *sud* mutants using

markers linked to *sud1-1* indicated that all four *sud* mutations were located in the same region, and targeted sequencing of the *SUD1* gene identified additional mutations on the three *sud* alleles. Thus, *dry2/sud1-2* caused a G360E substitution, *dry2/sud1-3* a R244K substitution, and *dry2/sud1-4* a premature stop codon at position 542 in the predicted SUD1 protein (Figure 3C and Supplemental Figure 2D). The identification of 4 independent *SUD1* mutant alleles in the suppressor screen demonstrates that mutations in the *SUD1* gene are responsible for the phenotypic recovery of the *dry2* defects.

SUD1 is homologous to E3 Ubiquitin ligases from yeast and mammals involved in ERAD

The Arabidopsis *SUD1* locus *AT4G34100* has been recently reported as *ECERIFERUM 9* (*CER9*), a gene involved in cuticular wax biosynthesis (Lu et al., 2012); still, to the best of our knowledge, no molecular mechanisms of SUD1 action has been reported in the literature. *SUD1* is predicted to encode a large protein of 1108 amino acids with a molecular weight of ~123-KDa. SUD1 contains a Really Interesting New Gene-variant (RING-v) domain (C4HC3 RING-finger domain) close to the N-terminus (Stone, 2005; Lu et al., 2012) and 14 putative transmembrane domains (Lu et al., 2012)(Figure 4A). The SUD1 RING-v domain shares high similarity to that of the E3 ubiquitin ligases TEB4 (57% amino acid identity), and Doa10 (49% amino acid identity). TEB4 and Doa10 are components of the Endoplasmic Reticulum Associated Protein Degradation (ERAD) complex involved in the quality control of ER proteins in human and yeast, respectively (Hassink et al., 2005; Kreft et al., 2006; Kreft and Hochstrasser, 2011). SUD1 also displays a high degree of similarity in an internal conserved segment of ~130 residues called TD (TEB4-Doa10) present in all Doa 10 orthologs (Swanson et al., 2001). Thus, the TD domain (transmembrane 5, 6 and 7) of SUD1 has a 45% and 31% amino acid identity to those of TEB4 and Doa10, respectively (Lu et al., 2012).

Next, we generated a topological model for SUD1 using sequence alignments and data from the experimental validation available for the homologous Doa10 (Kreft and Hochstrasser, 2011). For that purpose, we selected multiple SUD1 homologous proteins that complied with the following

criteria: (1) the conserved N-terminus RING-v domain, (2) the internal conserved TD domain, and (3) at least 10 predicted transmembrane (TM) domains (Swanson, 2001). As a result of the topological analysis, the N-terminus RING-v domain (and hence the putative ligase activity of SUD1) and the C-terminus were predicted to face the cytosol (Figure 4), a similar disposition to that of Doa10 (Kreft and Hochstrasser, 2011). This model was also used to locate the putative position of the amino acid residues affected in the different *sud1* mutant alleles. Thus, the mutations in the *sud1-1* and *sud1-2* alleles affected residues located at the transition between a TM domain and a hydrophilic loop. The mutation in *sud1-3* was located in the second cytosolic loop, and the mutation in *sud1-4* produced a premature stop codon at the end of TM5 domain (Figure 4B).

Additionally, an alignment between SUD1 and SUD1 homologous proteins of several plant species was performed using the plant comparative genomics resource PLAZA database (http://bioinformatics.psb.ugent.be/plaza/, (Proost et al., 2010). As shown in Supplemental Figure 3, the alignment of *Arabidopsis* SUD1 protein with the most homologous SUD1 proteins from several dicots (*Vitis vinifera*, *Populus trichocarpa*, *Medicago truncatula*, *Lotus japonicus*, *Glycine max*) and monocots (*Brachypodium distachyon*, *Oryza sativa* and *Zea mays*) showed striking sequence conservation. From the alignment we inferred that the amino acid substitutions in all suppressors occurred in conserved residues among monocots and dicots (Supplemental Figure 3).

Suppression of the *dry2* defects occurs without recovery in the composition of major sterols

dry2 and WT have similar sterol composition in shoots but significantly different sterol composition in roots (Posé et al., 2009) (Table 1). Since it has been proposed that the developmental defects in sterol biosynthetic mutants are the result of structural defects due to sterol depletions (Men et al., 2008; Babiychuk et al., 2008), we determined whether the suppression of *dry2* phenotypes was associated with a recovery in sterol content in roots. Sterol profiling using GC-MS analysis was performed separately in the shoots and roots of WT, *dry2*, and *dry2/sud1-1* seedlings. As shown in Table 1, WT, *dry2,*

and *dry2/sud1-1* shoots presented similar bulk sterol composition. In contrast, bulk sterol composition in *dry2/sud1-1* roots was similar to that of *dry2* and showed significant differences relative to WT. We therefore concluded that the reversion of the *dry2/sud1-1* root defects was not due to a recovery of major sterols to WT levels.

The recovery of the *dry2* defects by the *sud1-1* mutation without a recovery of sterol composition was further investigated by analyzing whether *sud1-1* was able to suppress the developmental defects of more severe sterol-deficient mutants. The selected mutants were *cpi1-1* that causes the loss-of-function of the *cyclopropylsterol isomerase gene* (Lovato et al., 2000; Men et al., 2008) and *fackel* that is mutated in a sterol C-14 reductase (Jang et al., 2000; Schrick et al., 2000). As shown in Supplemental Figure 4, no phenotypic recovery was observed when *sud1-1* was introduced in the *cpi1-1* and *fk-x224* mutants. These combined results support that the reversion of the *dry2* phenotype by *sud1* is not concomitant with changes on the sterol content.

A root-derived long-distance signal causes the *dry2* shoot phenotypic defects

Consistent with the identification of SQE1 as the main SQE enzyme in roots and with the sterol profiling results for *dry2* (Rasbery et al., 2007; Posé et al., 2009), we observed a dramatic accumulation of the substrate squalene in roots but not shoots of the *dry2* mutant (Table 1). Interestingly, *dry2/sud1-1* roots showed a significant reduction of squalene relative to *dry2* (Table 1), suggesting that *dry2* root defects could be caused by an accumulation of squalene and/or isoprenoid intermediates upstream of SQE1.

Since *dry2* shoots showed no differences in terms of bulk sterols or squalene accumulations with WT, we questioned whether squalene or other isoprenoid intermediate(s) generated in the *dry2* roots could move towards the shoots causing the observed phenotypes. In order to investigate this possibility, we performed micrografting experiments using WT, *dry2, and dry2/sud1-1* seedlings. The root and shoot of the grafted plants were genotyped by sequencing the corresponding *DRY2* and *SUD1* alleles. As expected, control grafted plants, i.e. L*er* scion/L*er* rootstock and *dry2* scion/*dry2* rootstock showed

WT and *dry2* phenotypes, respectively (Figure 5A). Importantly, *dry2* scion onto both, Ler rootstock (Figure 5A) and dry2/*sud1-1* rootstocks (Figure 5B) showed a WT phenotype, suggesting that a root-derived signal was causing the *dry2* shoot defects. Despite multiple attempts, we were unable to obtain a viable graft using WT or *sud1-1* scions onto *dry2* rootstocks. We therefore could not evaluate the effect of the *dry2* root-derived signal in healthy scions.

sud1 mutations suppress *dry2* root defects by down-regulating HMGR activity

It is known that in addition to the accumulation of squalene, the reduction of SQE activity causes a compensatory increase of HMGR activity (Wentzinger et al., 2002; Posé et al., 2009). As shown in Figure 6A, *dry2* roots increased the HMGR activity ~2 fold, while no differences were found in shoots. Importantly, in the roots of *dry2/sud1-1*, the HMGR activity returned to near WT levels, whereas in shoots HMGR activity decreased to ~0.7-fold that in shoots of both WT and *dry2* (Figure 6A).

To further investigate whether the reduction of HMGR activity could cause the recovery of the *dry2* roots we used atorvastatin, a specific inhibitor of HMGR activity. After testing several concentrations, we selected 10 nM atorvastatin. As shown in Figure 6B, this concentration did not have apparent effects in WT root growth or branching but substantially improved both phenotypes in *dry2*. This result supports that a reduction on the HMGR activity in *dry2/sud1-1* suppressor was responsible for the recovery of the *dry2* root phenotypic defects. We next treated WT, *dry2* and *dry2/sud1-1* seedlings with MVA, the product of the reaction catalyzed by HMGR. As shown in Figure 6C, a 5 mM MVA treatment caused a mild reduction on the WT root elongation while no visible changes were observed in *dry2* roots. However, the same treatment abolished the *sud1-1* suppressive effect of the *dry2* root defects, phenocoping *dry2* roots (Figure 6C). This result indicates that bypassing HMGR activity by adding the product of the HMGR reaction prevents the recovery of the *dry2* phenotype in a *dry2/sud1-1* background.

Genetic analysis on the regulation of HMGR activity by SUD1

To further investigate the link between HMGR activity and *SUD1*, the *dry2*/*sud1-1* mutant was crossed with transgenic lines overexpressing the catalytic domain of the HMGR1 (HMGR1-CD) and the short isoform of HMGR1 containing the TM domains (HMGR1S) (Supplemental Figure 5). HMGR1-CD and HMGR1S lines show a ~10-fold and ~3-fold increase in HMGR activity compared to WT, respectively (Manzano et al., 2004). As shown in Figure 7, the enhanced HMGR activity in a WT background only causes slight growth inhibition in the HMGR1-CD line and no visible effect in the HMGR1S line (Manzano et al., 2004). In contrast, the HMGR1-CD/*dry2* combination greatly enhanced the growth inhibition defects of *dry2* generating dwarf plants (Figure 7). The HMGR1S/*dry2* combination also showed enhanced growth inhibition compared to *dry2*, but less drastic than that observed in the HMGR1-CD/*dry2*. In fact viable seeds were obtained in this genotype while HMGR1-CD/*dry2* plants died before reaching maturity (Figure 7). These results indicate that the increase on HMGR activity in the presence of a *dry2* mutation accounts for the severity of the observed developmental phenotypes. Importantly, when the *sud1-1* mutation was introduced into HMGR-CD/*dry2* and HMGR1S/*dry2* there was an important recovery of the defective phenotypes to a point that HMGR-CD/*dry2/sud1-1* plants were fertile (Figure 7).

Based on these results, we propose a model in which the increase of HMGR activity concomitant to the reduction of SQE1 activity is mainly responsible for the observed developmental phenotypes in the *dry2* background. In this scenario, mutations on the positive regulator of HMGR *SUD1* cause the reversion of the *dry2* developmental defects by decreasing HMGR activity. An obvious question was whether the regulation of HMGR activity by SUD1 was dependent on the presence of the *dry2* mutation. Therefore the *sud1-1* mutation was segregated from *dry2* by backcrossing *dry2/sud1-1* to WT. As shown in Figure 8A, the single *sud1-1* mutant did not show any obvious phenotypic difference compared to WT plants, except by a glossy-like phenotype in shoots reminiscent of the phenotypes described for the loss-of-function *cer9-1* and *cer9-2* mutants allelic to *sud1* (Lu et al., 2012) Supplemental Figure 6. As shown in Figure 6A, HMGR activity in the *sud1-1* single mutant was ~0.75-fold lower than that of the WT in both shoots and roots,

indicating that *SUD1* is a positive regulator of HMGR activity acting independently of the *dry2* mutation.

Regulation of HMGR activity by SUD1 does not involved changes in protein content

Because SUD1 contains a RING-v domain putatively involved in ubiquitination (Stone, 2005), we used western blot analysis to investigate whether the regulation of HMGR activity mediated by SUD1 involves changes in HMGR protein content. The immunospecific antibodies used in the analysis were raised against the catalytic domain of HMGR1 (Manzano et al., 2004; Leivar et al., 2005). As shown in Figure 8B, the analysis of HMGR protein content in root samples revealed two bands of approximately 63 and 69 kDa corresponding to the HMGR1S and HMGR1L isoforms, respectively, whereas in shoot samples only the 63 kDa protein band was detected. In both cases, no significant differences in HMGR protein content among WT, *dry2*, *dry2/sud1-1* and *sud1-1* were observed (Figure 8B). This result, together with previous pharmacological studies reported (Wentzinger et al., 2002; Nieto et al., 2009) indicate that the variations in HMGR activity in the different genetic backgrounds occur without changes in the total HMGR protein content.

DISCUSSION

Mutations in the sterol biosynthetic *SQE1* gene produce multiple developmental defects, but in contrast to null alleles of *SQE1* (Rasbery et al., 2007), the hypomorphic *sqe1-5* allele is fully fertile (Posé at el., 2009). This characteristic lends itself to the use of *dry2/sqe1-5* as a genetic tool to identify processes that otherwise would be concealed. As a way to find new components regulating isoprenoid biosynthesis and/or signaling in *Arabidopsis* we performed a genetic screening for suppressors of *dry2*. Here we report the analysis of four suppressors and show that all mutations affect the *At4g34100* gene encoding a protein with a RING-variant domain, found in ubiquitin E3 ligases, subsequently named SUD1. Based on phylogenetic and structural similarities it is proposed that *SUD1* is an *Arabidopsis* orthologous protein of the yeast Doa10 and mammalian TEB4 involved in the ERAD-C pathway. Our physiological, molecular, biochemical, and genetic analyses strongly support that *sud1* recovers the *dry2* defects through the reversion of the enhanced HMGR activity of *dry2* to WT levels. Thus, our study uncovers *SUD1* as a novel regulator of HMGR activity in the plant isoprenoid biosynthetic pathway.

The accumulation of an MVA-derived signal in roots causes the *dry2* phenotypes

Despite its dramatic phenotypic defects, the sterol analysis of *dry2* showed only moderate changes in major bulk sterols in roots, and no significant changes in shoots compared to WT. Interestingly, the sterol analysis of *dry2/sud1-1* roots revealed a similar composition to that of *dry2* indicating that the *dry2* phenotypes cannot be simply explained by structural defects caused by the reduction in bulk sterols. Moreover, *dry2* shoots display WT characteristics when grafted onto WT rootstocks suggesting that a toxic mobile signal originated in the *dry2* roots is responsible for the observed *dry2* shoot phenotypes.

Although it is tempting to speculate that the squalene accumulated in *dry2* roots is the mobile signal responsible for the phenotypes, we argue against that notion because plants deal with excess squalene endogenously produced

or exogenously added by storing it as remobilizable cytosolic lipid droplets without obvious phenotypic defects (Wentzinger et al., 2002; Bouvier-Nave et al., 2009). Thus, we propose an alternative model whereby the accumulation of toxic intermediate(s), or derivative(s) acting upstream of squalene is responsible for the observed *dry2* developmental phenotypes. In fact, three independent experiments: (1) the inhibition of HMGR with atorvastatin that partially improved the *dry2* root defects, (2) the HMGR bypass with MVA that caused *dry2/sud1-1* (but not WT) to phenocopy *dry2*, and (3) the overexpression of HMGR that enhanced the *dry2* phenotypes, suggest that the *dry2* mobile signal(s) is not only triggered by the reduction of SQE1 activity but also by the concomitant up-regulation of the HMGR activity.

Supporting our model, the presence of toxic MVA-derived intermediates associated to HMGR activity changes has been reported in Insig-double-knockout mice that show developmental defects linked to enhanced HMGR activity (Engelking et al., 2006). As for *dry2*, the mice developmental defects were ameliorated with the use of HMGR inhibitors (Engelking et al., 2006). Interestingly, the Insig-knockout mice are not an isolated example. Non-sterol MVA-derived compounds upstream of squalene have been linked to the regulation of HMGR protein content in mammals, yeast, and plants. Thus, the degradation of mammalian HMGR is accelerated by the addition of farnesol, geranylgeraniol, and its precursor GGPP (Correll et al., 1994; Meigs et al., 1996; Räikkönen et al., 2010). GGPP is also known to regulate the degradation of HMGR2p in yeast (Garza et al., 2009). Surprisingly, the effect of farnesol on plant HMGR activity seems to be different than in mammals, because the addition of sub-toxic concentrations of farnesol to tobacco BY-2 cells had drastic stimulatory effect on HMGR activity (Hemmerlin and Bach, 2000).

Despite the similarities in the regulation of HMGR by a non-sterol MVA-derived molecule in different species, the regulatory mechanisms controlling HMGR activity in *Arabidopsis* operate at a different level than those in yeast and animals. Thus, our study and a previous report (Nieto et al., 2009) have shown that both genetic and pharmacological block of the Arabidopsis SQE activity leads to up-regulation of HMGR activity without changing HMGR protein amounts, while in yeast and animals HMGR activity depends on protein stability.

Structural characteristics of SUD1

All *sud1* alleles show a similar phenotypic recovery of *dry2* phenotypes, including *sud1-4* that is caused by a premature stop codon at the fifth transmembrane domain. The *sud1* alleles also show a glossy-like phenotype in leaves reminiscent to the *cer9* mutants in the same locus. Because *cer9* has been reported to be loss-of-function (Rashotte et al., 2004; Lu et al., 2012), and the allele *cer9-2* has the premature stop codon much more downstream than *sud1-4*, we presume that *sud1* are also loss-of-function alleles. Interestingly, the *cer9* alleles are recessive while all *sud1* alleles are semidominant with respect to the *dry2* mutation, which suggests that *SUD1* regulation of HMGR activity is dose-dependent. Thus, the heterozygous, *SUD1/sud1* genotype is unable to produce enough SUD1 protein to fully reproduce the *dry2* phenotypes.

The phylogenetic analysis and the structural features of the SUD1 suggest that this protein might function as one ortholog of the yeast Doa10 and human TEB4 in *Arabidopsis* (Kreft et al., 2006; Carvalho et al., 2006; Kreft and Hochstrasser, 2011), involved in the quality control that degrades misfolded ER proteins (Swanson, 2001). However, despite multiple attempts we failed to complement the yeast *doa10* mutant with SUD1 because this protein was highly unstable in yeast (data not shown). This result is not entirely surprising because complementation of the yeast *doa10* with TEB4 has also been unsuccessful despite them being proved to be orthologous proteins (Kreft et al., 2006).

When we analyze SUD1 plant homologs, we find a striking conservation of SUD1 sequence with homologous proteins from dicots and monocots. Indeed, amino acid substitutions in all suppressors occur in plant conserved residues. Thus, *sud1-1* and *sud1-2* result in G218R and G360E substitutions that change small non-polar residues for basic and acidic residues, respectively. Interestingly, both residues are located at the transition between a TM segment and a hydrophylic loop. Interruption of transmembrane helices by a short non-helical segment containing proline, glycine, and/or serine residues has also been observed in many classes of transporters, including amino-acid antiporters (Gao et al., 2009), neurotransmitter-sodium symporters (Yamashita et al., 2005), and sodium-independent transporters (Schulze et al., 2010). Interruption

of helical structures exposes main-chain carbonyl oxygen and nitrogen atoms for hydrogen bonding and ion coordination, aspects that are essential for proper function (Yamashita et al., 2005). The mutation in *sud1-3* results in the R244K substitution. These two amino acids are chemically related and it would be expected that its substitution did not cause important changes. However, phylogenetically distant plant species such as monocots and dicots maintain a conserved R around position 244, suggesting an important role for this specific residue in SUD1 function.

Regulation of HMGR activity by SUD1

A wealth of information about ERAD comes from yeast and mammals (Vembar and Brodsky, 2008; Smith et al., 2011). The HRD pathway (ERAD-L and ERAD-M) is involved in the degradation of misfolded ER-luminal and intramembrane domains; *HRD* genes were identified in a genetic screening for regulators of HMGR degradation (hence the name HRD, for HMGR Reductase Degradation) (Hampton et al., 1996). The finding that feedback regulation of sterol synthesis in mammalian and yeast cells uses the ERAD machinery (Hampton, 2002) illustrates co-option of the basic quality control mechanism for regulatory processes and reveals potential functions in cell-to-cell signaling. ERAD-regulated HMGR proteins such as those from yeast and mammals contain the known Sterol Sensing Domain (SSD) motif consisting of five consecutive TM spans (Theesfeld et al., 2001; Golstein et al., 2006). However, HMGR from plants contain 2 predicted TM domains (Supplemental Figure 5) (Campos and Boronat, 1995), therefore lacking any potential SSD motif. Surprisingly, following a non-targeted screening for plant HMGR regulators we identified SUD1, a likely ERAD component. Our first explanation was that HMGR stability was regulated by ERAD, either directly by SUD1 or through a compensatory increase of the HRD pathway in *sud1* mutants. However western-blot analyses indicated that SUD1 did not exert its function through control of HMGR proteins levels. Because SUD1 likely encodes an E3 ubiquitin ligase, another plausible explanation is that a negative regulator of HMGR is being degraded in a SUD1-dependent manner in *dry2*, so that the loss of SUD1

function would impair this degradation leading to the recovery of HMGR activity to WT levels.

Transcriptional versus Translational Regulation of HMGR.

It has been proposed that the major changes in HMGR activity in plants would be determined at the transcriptional level, whereas the posttranslational control would allow a finer and faster adjustment (Chappell, 1995). Whereas transcriptional modulation of HMGR has been demonstrated in many plant systems, evidence for regulatory mechanisms controlling HMGR activity at the posttranslational level is scarce. Thus, Nieto et al., (2009) have shown that metabolic perturbations by enhancing or depleting the flux through the sterol pathway in *Arabidopsis* causes a compensatory response in HMGR activity, without changes in transcript or protein levels; and Flores-Perez et al., (2010) has reported that the inactivation of the *Arabidopsis* WD protein PRL1 leads to reduced HMGR activity with no changes in transcript and protein levels. This effect could be related to the ability of PRL1 to interact and inhibit the activity of the Arabidopsis SNF1-related protein kinases (SnRK1) AKIN10 and AKIN11 (Bhalerao et al., 1999), presumably targeting them for ubiquitination and proteasomal degradation (Lee et al., 2008). Since plant SnRK1 phosphorylates and inactivates HMGR (Dale et al., 1995; Sugden et al., 1999) the loss of PRL1 function would result in increased SnRK1 activity followed by HMGR phosphorylation, and the subsequent reduction of HMGR activity. It has also been described that the HMGR activity is negatively regulated by PP2A-mediated dephosphorylation (Leivar et al., 2011). Therefore, the regulators of *Arabidopsis* HMGR activity SnRK1 and/or PP2A are candidates to act as mediators of the SUD1 regulation of HMGR activity. An alternative possibility is that SUD1 might produce the direct monoubiquitination of HMGR increasing its activity, as it has been reported for other proteins (Schnell and Hicke, 2003).

Overall, by using a genetic, physiological, biochemical and molecular approaches we show that SUD1, a likely component of the *Arabidopsis* ERAD-C pahtway**,** is a positive regulator of HMGR activity. Future research should help to clarify the mechanistic basis for the ERAD regulation of HMGR activity in plants and what signals are implicated in this regulation.

METHODS

Plant Material and Growth Conditions

Unless stated otherwise, the *Arabidopsis thaliana* plants used in this study were either grown on soil or petri dishes using an environmental chamber set for long-day lighting conditions (16 h light/8 h dark) and a temperature of 22 °C. For *in vitro* assays, surface-sterilized and cold-stratified *Arabidopsis* seeds were sown onto Murashige and Skoog phytagel-solidified medium (Murashige and Skoog salts, 30 g L^{-1} sucrose, and 7 g L^{-1} phytagel, pH 5.7). For chemical treatments, the appropriate amounts of filter sterilized chemical stock solutions were added to cooled autoclaved growth media. The *dry2* (Posé et al., 2009), *cpi1-1* (Schrick et al., 2000), *fk-x224* (Men et al., 2008) mutants, and the HMGR1-CD and HMGR1S overexpressing lines (Manzano et al., 2004) have been previously described.

Genetic screen for second-site suppressor mutations of *dry2*

dry2 seeds were mutagenized by imbibition in 75 mM ethylmethane sulfonate (EMS; Sigma) for 4 h at RT. After washing thoroughly with water for complete EMS removal, the mutagenized seeds (M_1) were sown on soil and grown under high humidity conditions. The M_2 seeds were harvested as 131 independent pools (each pool corresponding to 50 M1 plants). For the identification of *dry2* suppressors, the M_2 seeds were grown on soil under low watering conditions. Suppressors with enhanced drought tolerance compared to *dry2* plants were visually identified and selected for further analysis. Each candidate suppressor was genotyped using *DRY2* specific primers to confirm the presence of the *dry2* mutation. The primers sequences for genotyping were: DRY2 SEQ F, 5'-ATTGTTCTCGGTTGGGTGAG-3', DRY2 SEQ R, 5'-GATTGCAGTTCTCTAGGACCAA-3', and internal primer to sequence DRY2 SEQ2, 5'-TCAAAGAATGCGGGAGAAAG-3'.

Detection of Reactive Oxygen Species

Hydrogen peroxide was visually detected in leaves by using the 3,3´-diaminobenzidine DAB (Sigma) substrate as described previously (Orozco-Cardenas and Ryan, 1999). DAB was also used for *in situ* detection of hydrogen peroxide in roots from seedlings grown on phytagel-solidified medium (Carol et al., 2005). For *in situ* detection of superoxide in leaves the Nitroblue Tetrazolium (NBT Color Development Substrate, Promega) staining method (Jabs et al., 1996) was used. In all cases, stained leaves were imaged under dark-field illumination using a Leica *MZ FLII* stereomicroscope.

Whole-plant Stomatal Conductance and Determination of Proline Content

Leaf stomatal conductance to water vapour was measured using a Leaf Porometer Model SC-1 (Decagon Services) in 25-days-old leaves grown under short-day lighting conditions (8 h light/16 h dark). Measurements were performed after spraying the leaves with 0, 0.2, 2 and 20 µM of ABA (Sigma) dissolved in a 0.1% Tween20 solution. Proline was extracted and quantified as described previously (Borsani et al., 2002).

Root Measurements

Root measurements were performed according to the procedure described by Posé et al., (2009). Briefly, seeds were grown vertically on phytagel-solidified MS medium for 5 and 10 days for roots hairs and root elongation measurement, respectively. For root elongation assays, primary root lengths pictures were taken daily using a Nikon *Coolpix 4500* camera attached to a *MZ FLII* (Leica) stereomicroscope. Quantitative measurements were made using the Image J software (http://rsb.info.nih.gov/ij/). Root branching was determined by counting the number of root tips per length unit (cm) of primary root. Root hairs length was measured in the differentiation zone as described in Posé et al., (2009).

Identification of the *sud1-1* suppressor mutation

The *dry2* mutant in Landsberg background was crossed into the Col-0 ecotype for seven generations to generate a nearly isogenic *dry2*$^{Col-0}$ line for map-based

cloning. A F2 mapping population was created from a cross between the *dry2/sud1-1* (L*er*) and the introgressed *dry2*$^{Col-0}$ lines. 120 F2 plants displaying the suppression phenotypes conferred by the *dry2/sud1-1* mutations were used for rough mapping. For fine mapping, a total of 2,400 chromosomes were analyzed to locate *SUD1* locus into a 117-kb region at the bottom of chromosome IV with 36 candidate genes. All information regarding the genetic markers used in the map-based cloning was obtained from TAIR (http://www.arabidopsis.org/). The entire genome of *dry2/sud1-1* was sequenced using high throughput sequencing with the Illumina platform. Reads were filtered with Fastx-Toolkit software (http://hannonlab.cshl.edu/fastx_toolkit/index.html) and mapped with the *Arabidopsis* genome sequence version TAIR10 using the Burrows-Wheeler Alignment Tool (Li and Durbin, 2009). Polymorphisms for the 117-kb candidate region were analyzed with Samtools and Bcftools using regions with at least 5x depth coverage (Li et al., 2009), and filtered using the sequence information for the Landsberg ecotype available at 1001 Genomes (http://1001genomes.org/). After filtering, two non-synonymous mutations in the *AT4G34100* and *AT4G34135 loci* were identified. The identification of four independent suppressor alleles with mutations in the *AT4G34100* locus confirmed the identity of the *AT4G34100* locus as *SUD1.*

Informatic tools used for functional characterization of SUD1

The InterPro database (http://www.ebi.ac.uk/Tools/pfa/iprscan/) was used to search for conserved domains of SUD1 protein. The NCBI Blastp tool (http://blast.ncbi.nlm.nih.gov/Blast.cgi?PAGE=Proteins) was used to identify putative SUD1 orthologs, using the predicted proteome from *Saccharomyces cerevisiae* (taxid4932), *Homo sapiens* (taxid9606), *Mus musculus* (taxid10090), *Drosophila melanogaster* (taxid7227) and *Caenorhabditis elegans* (taxid6239).

The TMHMM2.0 program (www.cbs.dtu.dk/services/TMHMM/) was used to predict the putative TM domain topology of SUD1 based on the hydrophobicity plot (Krogh et al., 2001). The plant comparative genomics resource PLAZA (http://bioinformatics.psb.ugent.be/plaza/) was used to search for SUD1 homologous protein sequences in different plant species (Proost et

al., 2010). The protein sequence alignment of *Arabidopsis* SUD1 with homologous proteins from other plant species was performed with the software CLUSTALW2 available online on the European Bioinformatics Institute (http://www.ebi.ac.uk/Tools/msa/clustalw2/). All parameter values corresponded to default definitions (Gonnet Protein Weight Matrix, Gonnet et al., 1992).

Sterol and Squalene analysis and determination of HMGR activity

15-days-old seedlings grown in phytagel-solidified MS medium were used for sterol, squalene and HMGR activity measurements. A pool of ≥100 seedlings per genotype was used per each measurement. Since HMGR activity and isoprenoid biosynthesis are regulated by light conditions (Learned, 1996; Rodriguez-Concepcion, 2004), shoot and roots were collected and measured separately at 3 hours from the start of the light period. Quantification of total sterol content and determination of sterol profiles were performed as previously reported (Masferrer et al., 2002). HMGR activity was assayed as described (Nieto et al., 2009). In our assays, one unit of HMGR activity is defined as the amount of enzyme that converts one picomol of 3-hydroxy-3-methylglutaryl coenzyme A into MVA per min and mg of protein at 37^{o}C.

***Arabidopsis* grafting**

4-days-old seedlings grown vertically were transferred to a 0.22 μm sterile filter (Millipore) in contact with half-strength MS medium containing 0.6% (w/v) phytagel (Sigma). After three days, seedlings were grafted in sterile conditions in a wedge graft (Y shape) as described in Turnbull et al., (2002). Afterwards, the grafted plants were grown for seven additional days in humid conditions. Successful grafts were transferred to soil, and the grafting unions were confirmed by sequencing analysis of shoots and roots.

Determination of HMGR Protein Levels

HMGR protein levels were determined by immunoblot using a rabbit polyclonal antibody raised against the catalytic domain of Arabidopsis HMGR1 (Manzano et al., 2004; Leivar et al., 2005). The antibody was used at 1:1000 dilution and

the secondary antibody (horseradish peroxidase anti-rabbit IgG, Sigma) at 1:14000. For immunoblot analysis, total root and shoot protein were loaded in 10% acrilamide SDS gels. Immunoblot images were developed with Advanced ECL (GEHealthcare) and exposed to an X-ray film for 30 sec to 1 min. Coomassie brilliant blue staining was used to confirm equal loading.

Statistical analysis

Statistical analysis was performed using the STATGRAPHIC CENTURION program (Statpoint Technologies, Inc., Warrenton, Virginia, USA: www.statgraphics.com). The significance of differences was determined by ANOVA (for three or more samples) or a t-test (for two samples).

Accession Numbers

Arabidopsis Genome Initiative locus identifiers for the genes mentioned in this article are as follows: SQE1 (At1g58440), SUD1 (At4g34100), CPI1 (At5g50375), FK (At3g52940), and HMGR1 (At1g76490).

ACKNOWLEDGEMENTS

We thank Dr. Pedro Carvalho for helpful suggestions and Dr. Colin Turnbull for advice on grafting experiments. This work was supported by grants from Ministerio de Ciencia e Innovación (cofinanced by the European Regional Development Fund) to M.A.B. (BIO2011-23859 and CSD2007-00057), A.F. (BIO2009-06984 and CSD2007-00036), and O.B. from Universidad de la República-Comisión Sectorial de Investigación Científica (Grupo 418). V.G.D. was supported by FPI (Formación del Personal Investigador) fellowship from Ministerio de Educación y Ciencia (BIO2005-04733) and V.A-S. was supported by FCT (grant reference SFRH/BD/38583/2007).

AUTHOR CONTRIBUTIONS

V.G.D, V.A-S, performed research on the physiological, biochemical, and genetic data. D.P. identified the suppressors and performed an initial characterization. M.A. performed sterols and squalene analysis, and HMGR activity measurements. A.B. conducted the genomic analysis for *SUD1* identification. H.A. performed the ROS analyses. A.E. performed genetic crosses for *SUD1* identification. O.B. designed and performed the atorvastatin experiments. V.G.D., A.R., V.V., R.T. and M.A.B. designed the research. V.G.D., A.R., A.F. and M.A.B. wrote the article.

FIGURE LEGENDS

Figure 1. *dry2/sud1-1* and *dry2/sud1-2* suppress the shoot defects of *dry2*.

(A) Shoot phenotype of 3-weeks-old WT, *dry2*, *dry2/sud1-1* and *dry2/sud1-2* plants grown using standard LD conditions. Bar = 0.5 cm.

(B) Accumulation of O_2^- (upper panel) and H_2O_2 (lower panel) in 3-weeks-old leaves of WT, *dry2*, *dry2/sud1-1* and *dry2/sud1-2.* Plants were stained with NBT (upper panel) and DAB (lower panel). Compared to WT, *dry2/sud1-1* and *dry2/sud1-2*, *dry2* accumulates very low levels of O_2^- and H_2O_2. Bar = 0.5 cm.

(C) Stomatal conductance of WT, *dry2*, *dry2/sud1-1* and *dry2/sud1-2.* The measurements were made 4 hours after spraying the indicated ABA concentrations. The suppressors show wild-type stomatal responses to exogenous ABA compared to *dry2*.

(D) Proline content in WT, *dry2*, *dry2/sud1-1* and *dry2/sud1-2* plants grown at 35% and 90% Relative Humidity.

(C) and (D) Mean ± SD, *n* = 9; values with the same letter are not significantly different at $P < 0.05$. The experiments were repeated at least three times with similar results.

Figure 2. The *dry2/sud1* mutants partially suppress the root elongation and root hair growth defects of the *dry2* mutant.

(A) Root developmental phenotypes of 10-days-old WT, *dry2*, *dry2/sud1-1* and *dry2/sud1-2* mutant seedlings. Bar = 1 cm.

(B) Primary root growth during a 10-day time lapse for WT, *dry2*, *dry2/sud1-1* and *dry2/sud1-2*. $n \geq 30$ roots per genotype.

(C) Root branching index for 10-days-old WT, *dry2, dry2/sud1-1* and *dry2/sud1-2.* The index was determined by counting the number of lateral root tips per length unit (cm) of primary root. *n* = 30 roots counted per genotype. Values with the same letter are not significantly different at $P < 0.05$.

(D) Root hairs length distribution in 5-days-old WT, *dry2*, *dry2/sud1-1* and *dry2/sud1-2* (*n* ≥ 300 root hairs counted in a total of 30 roots per genotype).

(E) Morphologic root hair phenotype in 5-days-old WT, *dry2*, *dry2/sud1-1* and *dry2/sud1-2*. Bar = 500 μm.

(F) ROS staining in 5-days-old roots using DAB. H_2O_2 (arrows) is localized at the tips of WT, *dry2/sud1-1* and *dry2/sud1-2* root hairs, but not in *dry2*. Bar = 200 μm.

Figure 3. Genetic analyses of *dry2/sud1-1* and *dry2/sud1-2*.

(A) Visual score of the phenotypes from the F1 of the corresponding crosses

(B) Phenotypes of WT, *dry2*, *dry2/sud1-1* and a F1 plant derived from the backcross between a *dry2/sud1-1* and a *dry2* plant is shown. Bar = 2 cm.

(C) The four suppressor mutations are localized in the *AT4G34100* gene. The intron/exon structure of the gene, the position of the mutations and the resulting amino acids substitution of the four suppressors is depicted.

Figure 4. Topology model for SUD1 protein.

(A) Topology of *Arabidopsis* SUD1 predicted by TMHMM2.0. The 14 TM segments are depicted as numbered small red boxes near the top; lines connected to the bottom edge of these boxes represent cytosolic loops, and those connected to the top edges depict luminal loops.

(B) The 14 transmembrane (TM) domains of SUD1 are numbered and represented by green cylinders and are the result of the TMHMM2.0 prediction shown in (A). Both protein termini are represented facing the cytosol based on the experimentally determined Doa10 topology (Kreft et al., 2006). The amino acid substitution of a given *sud1* allele is depicted as a green circle. Positions of the amino acid substitutions and the protein variants are indicated. The RING□v domain (residues 68□115) at the N terminus is shown as a black cylinder and the conserved TD domain (residues 524□654) is highlighted by gray shading.

Figure 5. Suppression of *dry2* shoot (scion) defects by WT and *dry2/sud1-1* rootstocks. A total of 20 viable plants per graft combination were analyzed and a representative plant per combination is depicted 18 days after growing in soil. Lower panels show the plants after soil removal to visualize the root phenotype. Scale bar = 2 cm.

(A) *dry2* shoot (scion) recovers the WT phenotype when grafted onto WT L*er* rootstock. Self-grafted WT (L*er*) and *dry2* were used as controls.

(B) *dry2* shoot (scion) recovers the WT phenotype when grafted onto

dry2/sud1-1 rootstock. Self-grafted *dry2/sud1-1* and *dry2* were used as controls.

Figure 6. HMGR activity changes correlate with the phenotypes observed in *dry2* and *dry2/sud1-1*.

(A) HMGR activity measurement in roots and shoots of 15-day-old WT, *dry2*, *dry2/sud1-1* and *sud1-1* seedlings (mean ± SD, *n* = 3; each measure corresponds to a pool of ≥ 100 seedlings). Values with the same letter are not significantly different at $P < 0.05$. The experiment was repeated at least three times with similar results.

(B) Inhibition of HMGR activity partially recovers *dry2* roots defects. WT and *dry2* seeds were germinated and grown on MS plates for 4 days. Seedlings were then transferred to MS supplemented with 10 nM of the HMGR inhibitor atorvastatin and grown for additional 2 weeks (mean ± SD, *n* = 30; values with the same letter are not significantly different at $P < 0.05$). The experiment was repeated three times with similar results. Bar = 1 cm.

(C) *dry2/sud1-1* roots phenocopy *dry2* in the presence of MVA. WT, *dry2* and *dry2/sud1-1* were germinated and grown on MS plates for 4 days. Seedlings were then transferred to MS supplemented with MVA and grown for 2 additional weeks (mean ± SD, *n* = 30; values with the same letter are not significantly different at $P < 0.05$). The experiment was repeated three times with similar results. Bar = 1 cm.

Figure 7. Phenotypic analysis of plants overexpressing *HMGR1S* (1S) and *HMGR1-CD* (CD) in *dry2* and *dry2/sud1-1* backgrounds. The WT, *dry2* and *dry2/sud1-1* plants are in background L*er* ecotype. The transgenic HMGR1-CD or HMGR1S plants are in Col glabrous background. The resulting F2 from the crosses are Col-Ler hybrids. Plants were grown for 3 weeks on soil under LD conditions. All plants were fertile with the exception of CD/*dry2* plants. Bar = 1 cm.

Figure 8. *sud1-1* mutation produces no visible phenotype and no changes in HMGR protein content.

(A) Phenotype of WT, *dry2*, *dry2/sud1-1* and *sud1-1* seedlings grown for 15 days on MS medium under LD conditions. Scale bar = 1 cm.

(B) Western-blot analysis of HMGR protein in 15-day-old roots and shoots of WT, *dry2*, *dry2/sud1-1* and *sud1-1*. Intensities of the HMGR protein bands (upper panel) and the Coomassie blue stained gel (lower panel) were quantified using *ImageJ* software (http://rsb.info.nih.gov/ij). The normalized HMGR protein levels expressed as relative abundance to the amount of the HMGR1S isoform in WT plants (arbitrarily set at 1) is shown at the top of each lane. Image shows the result from one representative experiment. Four independent experiments with similar results were performed.

Table 1. Mass spectral analysis of sterols and squalene from WT, *dry2* and *dry2/sud1-1*

Sterol	Root			Shoot		
	WT	*dry2*	*dry2/sud1-1*	WT	*dry2*	*dry2/sud1-1*
Cycloartenol	37±6[a]	104 ± 22[b]	82±23[b]	28±2[a]	28±6[a]	26±5[a]
24-Methylenecycloartenol	46±1[a]	86±12[b]	102±8[b]	48±2[a]	44±3[a]	47±9[a]
Isofucosterol	63±4[a]	41±9[a]	51±25[a]	63±3[a]	69±4[a]	66±13[a]
Sitosterol	2579±144[b]	1518±58[a]	1617±91[a]	2234±101[ab]	2052±34[a]	2302±148[b]
Stigmasterol	904±10[b]	304±53[a]	317±19[a]	60±3[a]	65±13[a]	69±6[a]
Campesterol	407±3[ab]	499±75[b]	263±107[a]	422±27[a]	439±38[a]	423±50[a]
Cholesterol	32±12[a]	18±6[a]	24±7[a]	46±4[a]	45±1[a]	48±4[a]
Squalene	**10±4[a]**	**1206±207[b]**	**75±13[a]**	**10±2[a]**	**15±4[a]**	**13±5[a]**

Values are given in μg g^{-1} dry weight.
Mean ± SD, *n* = 3; values with the same letter are not significantly different at $P < 0.05$.

REFERENCES

Babiychuk, E., Bouvier-Navé, P., Compagnon, V., Suzuki, M., Muranaka, T., Montagu, M.V., Kushnir, S., and Schaller, H. (2008). Allelic mutant series reveal distinct functions for *Arabidopsis* cycloartenol synthase 1 in cell viability and plastid biogenesis. Proc. Natl. Acad. Sci. USA **105**: 3163–3168.

Benveniste, P. (2004). Biosynthesis and accumulation of sterols. Annu. Rev. Plant Biol. **55**: 429–457.

Bhalerao, R.P., Salchert, K., Bakó, L., Ökrész, L., Szabados, L., Muranaka, T., Machida, Y., Schell, J., and Koncz, C. (1999). Regulatory interaction of PRL1 WD protein with *Arabidopsis* SNF1-like protein kinases. Proc. Natl. Acad. Sci. USA **96**: 5322–5327.

Borsani, O., Cuartero, J., Valpuesta, V., and Botella, M.A. (2002). Tomato *tos1* mutation indentifies a gene essential for osmotic tolerance and abscisic acid sensitivity. Plant J. **32**:905–914.

Boutté, Y., and Grebe, M. (2009). Cellular processes relying on sterol function in plants. Curr. Opin. Plant Biol. **12**: 705–713.

Bouvier, F., Rahier, A., and Camara, B. (2005). Biogenesis, molecular regulation and function of plant isoprenoids. Prog. Lipid Res. **44**: 357–429.

Bouvier-Nave, P., Berna, A., Noiriel, A., Compagnon, V., Carlsson, A.S., Banas, A., Stymne, S., and Schaller, H. (2009). Involvement of the phospholipid sterol Acyltransferase1 in plant sterol homeostasis and leaf senescence. Plant Physiol. **152**: 107–119.

Brodersen, P., Sakvarelidze-Achard, L., Schaller, H., Khafif, M., Schott, G., Bendahmane, A., and Voinnet, O. (2012). Isoprenoid biosynthesis is required for miRNA function and affects membrane association of ARGONAUTE 1 in *Arabidopsis*. Proc. Natl. Acad. Sci. USA **109**: 1778-1783.

Campos, N., and Boronat, A. (1995). Targeting and topology in the membrane of plant 3-hydroxy-3-methylglutaryl coenzyme A reductase. Plant Cell **7**:2163–2174.

Carland, F., Fujioka, S., and Nelson, T. (2010). The Sterol Methyltransferases SMT1, SMT2, and SMT3 influence *Arabidopsis* development through nonbrassinosteroid products. Plant Physiol. **153**: 741–756.

Carol, R.J., Takeda, S., Linstead, P., Durrant, M.C., Kakesova, H., Derbyshire, P., Drea, S., Zarsky, V., and Dolan, L. (2005). A RhoGDP dissociation inhibitor spatially regulates growth in root hair cells. Nature **438:**1013-1016.

Carvalho, P., Goder, V., and Rapoport, T.A. (2006). Distinct Ubiquitin-Ligase complexes define convergent pathways for the degradation of ER proteins. Cell **126**: 361–373.

Chappell, J. (1995). The biochemistry and molecular biology of isoprenoid metabolism. Plant Physiol. **107**: 1–6.

Correll, C.C., Ng, L,, and Edwards, P.A. (1994). Identification of farnesol as the non-sterol derivative of mevalonic acid required for the accelerated degradation of 3-Hydroxy-3-methylglutaryl-Coenzyme A Reductase. J. Biol. Chem. **269**: 17390–17393.

Dale, S., Arró, M., Becerra, B., Morrice, N.G., Borona, A., Hardie, D.G., and Ferrer, A. (1995). Bacterial expression of the catalytic domain of 3–Hydroxy-3–Methylglutaryl-CoA Reductase (isoform HMGR1) from *Arabidopsis thaliana*, and its inactivation by phosphorylation at Ser577 by *Brassica oleracea* 3-Hydroxy-3-Methylglutaryl-CoA Reductase Kinase. Eur. J. Biochem. **233**: 506–513.

Eisenreich, W., Rohdich, F., and Bacher, A. (2001). Deoxyxylulose phosphate pathway to terpenoids. Trends Plant Sci. **6**: 78–84.

Engelking, L.J., Evers, B.M., Richardson, J.A., Goldstein, J.L., Brown, M.S., and Liang, G. (2006). Severe facial clefting in Insig-deficient mouse embryos caused by sterol accumulation and reversed by lovastatin. J. Clinical Investigation **116**: 2356-2365.

Enjuto, M., Balcells, L., Campo, N., Caelles, C., Arró, M., and Boronat, A. (1994). *Arabidopsis thaliana* contains two differentially expressed *3-hydroxy-3-methylglutaryl-CoA reductase* genes, which encode microsomal forms of the enzyme. Proc. Natl. Acad. Sci. USA **91**: 927–931.

Flores-Perez, U., Perez-Gil, J., Closa, M., Wright, L.P., Botella-Pavia, P., Phillips, M.A., Ferrer, A., Gershenzon, J., and Rodriguez-Concepcion, M. (2010). Pleiotropic Regulatory Locus 1 (PRL1) integrates the regulation of sugar responses with Isoprenoid metabolism in *Arabidopsis*. Molecular Plant **3**: 101–112.

Gao, X., Lu, F., Zhou, L., Dang, S., Sun, L., Li, X., Wang, J., and Shi, Y. (2009). Structure and mechanism of an amino acid antiporter. Science **324**: 1565–1568.

Garza, R.M., Tran, P.N., and Hampton, R.Y. (2009). Geranylgeranyl Pyrophosphate is a potent regulator of HRD-dependent 3-Hydroxy-3-methylglutaryl-CoA Reductase degradation in yeast. J. Biol. Chem. **284**: 35368–35380.

Goldstein, J.L., DeBose-Boyd, R.A., and Brown, M.S. (2006). Protein sensors for membrane sterols. Cell Review 35-46.

Gonnet, G.H., Cohen, M.A., and Benner, S.A. (1992). Exhaustive matching of the entire protein sequence database. Science **256**: 1443–1445.

Hampton, R.Y., Gardner, R.G., and Rine, J. (1996). Role of 26S proteasome and *HRD* genes in the degradation of 3-hydroxy-3-methylglutaryl-CoA reductase, an integral endoplasmic reticulum membrane protein. Mol. Bio. Cell **7**:2029–2044.

Hampton, R.Y. (2002). ER-associated degradation in protein quality control and cellular regulation. Curr. Opin. Cell Biol. **14**: 476–482.

Hassink, G., Kikkert, M., Voorden, S.V., Lee, S.-J., Spaapen, R., Laar, T.V., Coleman, C.S., Bartee, E., Früh, K., Chaus, V., and Wiertz, E. (2005). TEB4 is a C4HC3 RING finger-containing ubiquitin ligase of the endoplasmic reticulum. Biochem J. **388**: 647–655.

Hemmerlin, A., and Bach, T.J. (2000). Farnesol-induced cell death and stimulation of 3-Hydroxy-3-Methylglutaryl-Coenzyme A Reductase activity in tobacco cv Bright Yellow-2 cells. Plant Physiol. **123**: 1257–1268.

Hemmerlin, A., Harwood, J.L., and Bach, T.J. (2012). A raison *d´être* for two distinct pathways in the early steps of plant isoprenoid biosynthesis? Prog. Lipid Res. **51**: 95–148.

Jabs, T., Dietrich, R.A., and Dang, J.L. (1996). Initiation of runaway cell death in an *Arabidopsis* mutant by extracellular Superoxide. Science **273**: 1853–1856.

Jang, J.-C., Fujioka, S., Tasaka, M., Seto, H., Takatsuto, S., Ishii, A., Aida, M., Yoshida, S., and Sheen, J. (2000). A critical role of sterols in embryonic patterning and meristem programming revealed by the *fackel* mutants of *Arabidopsis thaliana*. Genes Dev. **14**: 1485–1497.

Koornneef, M., Alonso-Blanco, C., and Stam, P. (2006). Genetic analysis. Methods Mol. Biol. **323**: 65–77.

Kreft, S.G., and Hochstrasser, M. (2011). An unusual transmembrane helix in the Endoplasmic Reticulum Ubiquitin Ligase Doa10 modulates degradation of its cognate E2 enzyme. J. Biol. Chem. **286**: 20163–20174.

Kreft, S.G., Wang, L., and Hochstrasser, M. (2006). Membrane topology of the yeast endoplasmic reticulum-localized Ubiquitin Ligase Doa10 and comparison with its human ortholog TEB4 (MARCH-VI). J. Biol. Chem. **281**: 4646–4653.

Krogh, A., Larsson, B., Heijne von, G., and Sonnhammer, E.L.L. (2001). Predicting transmembrane protein topology with a hidden markov model: application to complete genomes1. J. Mol. Biol. **305**: 567–580.

Learned, R.M. (1996). Light suppresses 3-Hydroxy-3-methylglutaryl Coenzyme A Reductase gene expression in *Arabidopsis thaliana*. Plant Physiol. **110**:645–655.

Lee, J.H., Terzaghi, W., Gusmaroli, G., Charron, J.B.F., Yoon, H.J., Chen, H., He, Y.J., Xiong, Y., and Deng, X.W. (2008). Characterization of *Arabidopsis* and rice DWD proteins and their roles as substrate receptors for CUL4-RING E3 Ubiquitin Ligases. Plant Cell **20**: 152–167.

Leivar, P., **González, V.M., Castel, S., Trelease, R.N., López-Iglesias, C., Arró, M., Boronat, A., Campos, N., Ferrer, A., and Fernández-Busquets, X.** (2005). Subcellular localization of *Arabidopsis* 3-Hydroxy-3-Methylglutaryl-

Coenzyme A Reductase. Plant Physiol. **137**: 57–69.

Leivar, P., Antolin-Llovera, M., Ferrero, S., Closa, M., Arró, M., Ferrer, A., Boronat, A., and Campos, N. (2011). Multilevel control of *Arabidopsis* 3-Hydroxy-3-Methylglutaryl Coenzyme A Reductase by Protein Phosphatase 2A. Plant Cell **23**: 1494–1511.

Li, H., and Durbin, R. (2009). Fast and accurate short read alignment with Burrows-Wheeler transform. Bioinformatics **25**: 1754–1760.

Li, H., Handsaker, B., Wysoker, A., Fennell, T., Ruan, J., Homer, N., Marth, G., Abecasis, G., Durbin, R., and 1000 Genome Project Data Processing Subgroup (2009). The sequence alignment/map format and SAMtools. Bioinformatics **25**: 2078–2079.

Lovato, M.A., Hart, E.A., Segura, M.J.R., Giner, J.-L., and Matsuda, S.P.T. (2000). Functional cloning of an *Arabidopsis thaliana* cDNA encoding cycloeucalenol cycloisomerase. J. Biol. Chem. **275**: 13394–13397.

Lu, S., Zhao, H., Marais Des, D.L., Parsons, E.P., Wen, X., Xu, X., Bangarusamy, D.K., Wang, G., Rowland, O., Juenger, T., Bressan, R.A., and Jenks, M.A. (2012). *Arabidopsis* ECERIFERUM9 involvement in cuticle formation and maintenance of plant water status. Plant Physiol.**159**: 930-944.

Lumbreras, V., Campos, N., and Boronat, A. (1995). The use of an alternative promoter in the *Arabidopsis thaliana HMG1* gene generates an mRNA that encodes a novel 3-hydroxy-3-methylglutaryl coenzyme A reductase isoform with an extended N-terminal region. Plant J. **8**: 541–549.

Manzano, D., Fernández-Busquets, X., Schaller, H., González, V.C., Boronat, A., Arró, M., and Ferrer, A. (2004). The metabolic imbalance underlying lesion formation in Arabidopsis thaliana overexpressing farnesyl diphosphate synthase (isoform 1S) leads to oxidative stress and is triggered by the developmental decline of endogenous HMGR activity. Planta **219**: 982–992.

Masferrer, A., Arró, M., Manzano, D., Schaller, H., Fernández-Busquets, X., Moncaleán, P., Fernández, B., Cunillera, N., Boronat, A., and Ferrer, A. (2002). Overexpression of *Arabidopsis thaliana* farnesyl diphosphate synthase (FPS1S) in transgenic *Arabidopsis* induces a cell death/senescence-like rsponse and reduced cytokinin levels. Plant J. **30**: 123–132.

McGarvey, D.J., and Croteau, R. (1995). Terpenoid Metabolism. Plant Cell **7**: 1015–1026.

Meigs, T.E., Roseman, D., and Simoni, R.D. (1996). Regulation of 3-3Hydroxy-3-methylglutaryl-Coenzyme A Reductase degradation by the nonsterol mevalonate metabolite farnesol *in Vivo*. J. Biol. Chem. **271**: 7916–7922.

Men, S., Boutté, Y., Ikeda, Y., Li, X., Palme, K., Stierhof, Y.-D., Hartmann, M.-A., Moritz, T., and Grebe, M. (2008). Sterol-dependent endocytosis mediates post-cytokinetic acquisition of PIN2 auxin efflux carrier polarity. Nat

Cell Biol **10**: 237–244.

Newman, J.D., and Chappell, J. (1999). Isoprenoid biosynthesis in plants: carbon partitioning within the cytoplasmic pathway. Crit. Rev. Biochem. Mol. Biol. **34**: 95–106.

Nicotra, A.B., Atkin, O.K., Bonser, S.P., Davidson, A.M., Finnegan, E.J., Mathesius, U., Poot, P., Purugganan, M.D., Richards, C.L., Valladares, F., and van Kleunen, M. (2010). Plant phenotypic plasticity in a changing climate. Trends Plant Sci. **15**: 684–692.

Nieto, B., Forés, O., Arró, M., and Ferrer, A. (2009). Arabidopsis 3-hydroxy-3-methylglutaryl-CoA reductase is regulated at the post-translational level in response to alterations of the sphingolipid and the sterol biosynthetic pathways. Phytochemistry **70**: 53–59.

Orozco-Cardenas, M., and Ryan, C.A. (1999). Hydrogen peroxide is generated systemically in plant leaves by wounding and systemin via the octadecanoid pathway. Proc. Natl. Acad. Sci. USA **96**: 6553–6557.

Ossowski, S., Schneeberger, K., Clark, R.M., Lanz, C., Warthmann, N., and Weigel, D. (2008). Sequencing of natural strains of *Arabidopsis thaliana* with short reads. Genome Res. **18**: 2024–2033.

Phillips, D.R., Rasbery, J.M., Bartel, B., and Matsuda, S.P. (2006). Biosynthetic diversity in plant triterpene cyclization. Curr. Opin. Plant Biol. **9**: 305–314.

Posé, D., Castanedo, I., Borsani, O., Nieto, B., Rosado, A., Taconnat, L., Ferrer, A., Dolan, L., Valpuesta, V., and Botella, M.A. (2009). Identification of the *Arabidopsis dry2/sqe1-5* mutant reveals a central role for sterols in drought tolerance and regulation of reactive oxygen species. Plant J. **59**: 63–76.

Proost, S., Van Bel, M., Sterck, L., Billiau, K., Van Parys, T., Van de Peer, Y., and Vandepoele, K. (2010). PLAZA: a comparative genomics resource to study gene and genome evolution in plants. Plant Cell **21**: 3718–3731.

Rasbery, J.M., Shan, H., LeClair, R.J., Norman, M., Matsuda, S.P.T., and Bartel, B. (2007). *Arabidopsis thaliana* Squalene Epoxidase 1 is essential for root and seed development. J. Biol. Chem. **282**: 17002–17013.

Rashotte, A.M., Jenks, M.A., Ross A.S., and Feldmann, K.A. (2004). Novel eceriferum mutants in *Arabidopsis thaliana*. Planta **219**: 5-13.

Räikkönen, J., Mönkkönen, H., Auriola, S., and Mönkkönen, J. (2010). Mevalonate pathway intermediates downregulate zoledronic acid-induced isopentenyl pyrophosphate and ATP analog formation in human breast cancer cells. Biochem. Pharm. **79**: 777–783.

Rodriguez-Concepcion, M. and Boronat, A. (2002). Elucidation of the methylerythritol phosphate pathway for isoprenoid biosynthesis in bacteria and plastids. A metabolic milestone achieved through genomics. Plant Physiol. **130**:

1079–1089.

Rodriguez-Concepcion, M. (2004). Distinct Light-Mediated Pathways Regulate the Biosynthesis and Exchange of Isoprenoid Precursors during *Arabidopsis* Seedling Development. Plant Cell **16**:144–156.

Schaller, H. (2010). Sterol and steroid biosynthesis and metabolism in plants and microorganisms. Comprehensive Natural Products II Chemistry and Biology **1**: 755–787.

Schnell, J.D. and Hicke, L. (2003). Non-traditional functions of ubiquitin and ubiquitin-binding proteins. J. Biol. Chem. **278**: 35857–35860.

Schrick, K., Fujioka, S., Takatsuto, S., Stierhof, Y.-D., Stransky, H., Yoshida, S., and Jürgen,s G. (2004). A link between sterol biosynthesis, the cell wall, and cellulose in *Arabidopsis*. Plant J. **38**: 227–243.

Schrick, K., Mayer, U., Horrichs, A., Kuhnt, C., Bellini, C., Dangl, J., Schmidt, J., and Jürgens, G. (2000). FACKEL is a sterol C-14 reductase required for organized cell division and expansion in *Arabidopsis* embryogenesis. Genes Dev. **14**: 1471-1484.

Smith, M.H., Ploegh, H.L., and Weissman, J.S. (2011). Road to ruin: targeting proteins for degradation in the endoplasmic reticulum. Science **334**: 1086–1090.

Stone, S.L. (2005) Functional Analysis of the RING-Type Ubiquitin Ligase Family of Arabidopsis. Plant Physiol. **137**:13–30.

Sugden, C., Donaghy, P.G., Halford, N.G., and Hardie, D.G. (1999). Two SNF1-related protein kinases from spinach leaf phosphorylated and inactive 3-Hydroxy-3-Methylglutaryl-Coenzyme A Reductase, Nitrate Reductase, and Sucrose Phosphate Synthase *in vitro*. Plant Physiol. **120**: 257–274.

Suzuki, M., Kamide, Y., Nagata, N., Seki, H., Ohyama, K., Kato, H., Masuda, K., Sato, S., Kato, T., Tabata, S., Yoshida, S., and Muranaka, T. (2004). Loss of function of *3-hydroxy-3-methylglutaryl coenzyme A reductase 1* (*HMG1*) in *Arabidopsis* leads to dwarfing, early senescence and male sterility, and reduced sterol levels. Plant J. **37**: 750–761.

Suzuki, M., Nakagawa, S., Kamide, Y., Kobayashi, K., Ohyama, K., Hashinokuchi, H., Kiuchi, R., Saito, K., Muranaka, T., and Nagata, N. (2009). Complete blockage of the mevalonate pathway results in male gametophyte lethality. J. Exp. Bot. **60**: 2055–2064.

Swanson, R., Locher, M., and Hochstrasser, M. (2001). A conserved ubiquitin ligase of the nuclear envelope/endoplasmic reticulum that functions in both ER-associated and Mat∝ 2 repressor degradation. Genes Dev. **15**: 2660–glutaryl (HMG)-CoA reductase isozyme Hmg2p. J. Biol. Chem. **286**: 26298-26307.

Theesfeld, C.L., Pourmand, D., Davis, T., Garza, R.M., and Hampton R.Y.

(2011). The sterol-sensing domain (SSD) directly mediates signal-regulated endoplasmic reticulum-associated degradation (ERAD) of 3-hydroxy-3-methyl

Tholl, D., and Lee, S. (2011). Terpene specialized metabolism in *Arabidopsis thaliana*. Arabidopsis Book.

Turnbull, C.G.N., Booker, J.P., and Ottoline Leyser, H.M. (2002). Micrografting techniques for testing long-distance signalling in *Arabidopsis*. Plant J. **32**:255–262.

Vembar, S.S., and Brodsky, J.L. (2008). One step at a time: endoplasmic reticulum-associated degradation. Nat. Rev. Mol. Cell Biol. **9**: 944–957.

Wentzinger, L.Ff, Bach, T.J., and Hartmann, M.-A. (2002). Inhibition of Squalene Synthase and Squalene Epoxidase in tobacco cells triggers an up-Regulation of 3-Hydroxy-3-Methylglutaryl Coenzyme A Reductase. Plant Physiol. **130**: 334–346.

Willemsen, V., Grebe, M., van den Toorn, A., Palme, K., and Scheres, B. (2003). Cell Polarity and PIN Protein Positioning in *Arabidopsis* Require Sterol Methyltransferase1 Function. Plant Cell **15**: 612–625.

Yamashita, A., Singh, S.K., Kawate, T., Jin, Y., and Gouaux, E. (2005). Crystal structure of a bacterial homologue of Na+/Cl--dependent neurotransmitter transporters. Nat. Cell Biol. **437**: 215–223.


A
WT
dry2
dry2/sud1-1
dry2/sud1-2

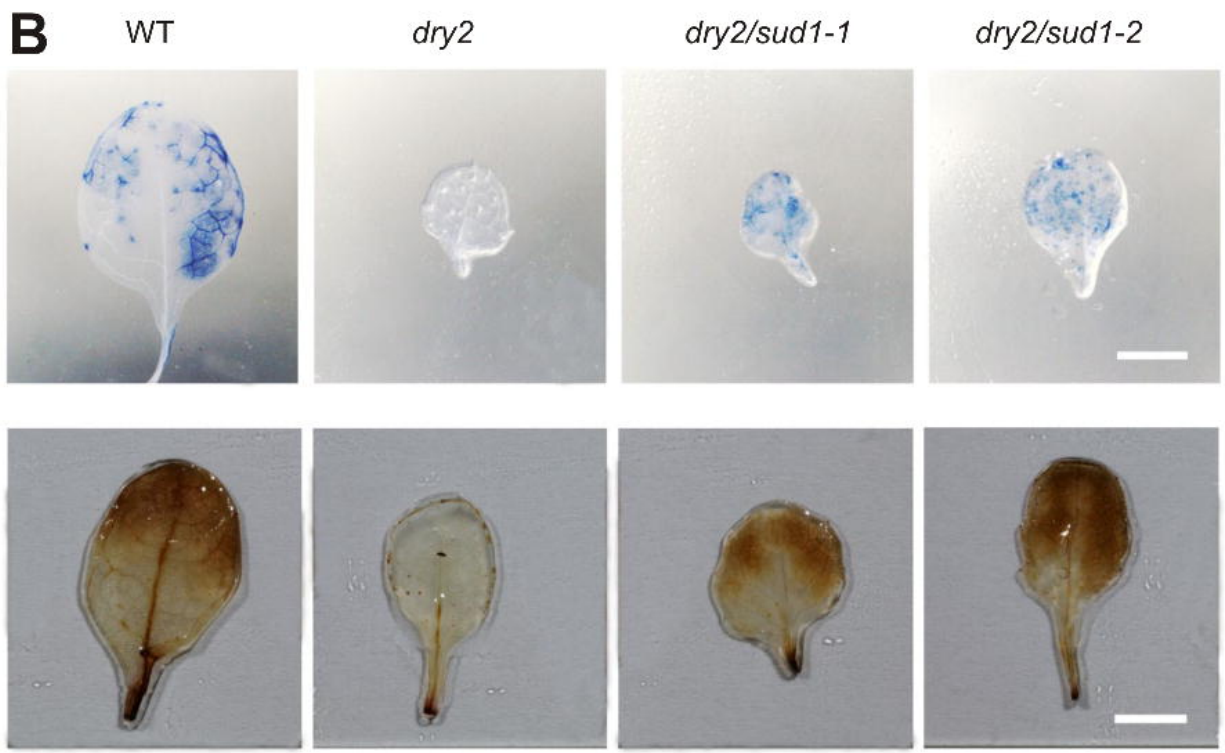
B
WT
dry2
dry2/sud1-1
dry2/sud1-2

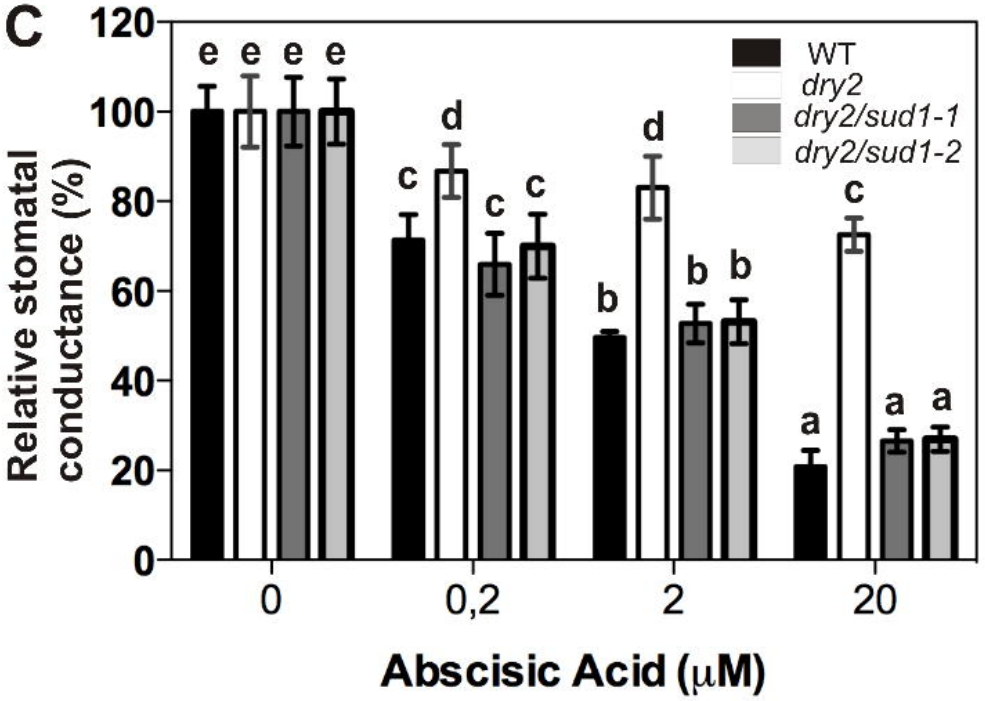
C
Relative stomatal conductance (%)
120
100
80
60
40
20
0
e e e e
c d c c
b d b b
a c a a
WT
dry2
dry2/sud1-1
dry2/sud1-2
0
0,2
2
20
Abscisic Acid (μM)

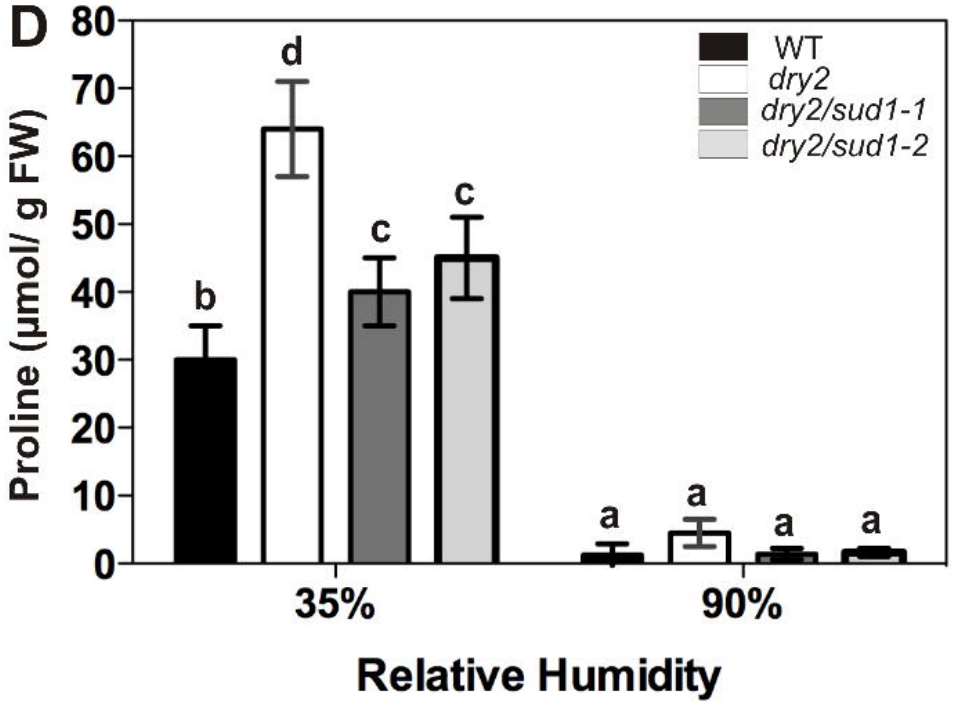
D
Proline (μmol/ g FW)
80
70
60
50
40
30
20
10
0
b d c c
a a a a
WT
dry2
dry2/sud1-1
dry2/sud1-2
35%
90%
Relative Humidity

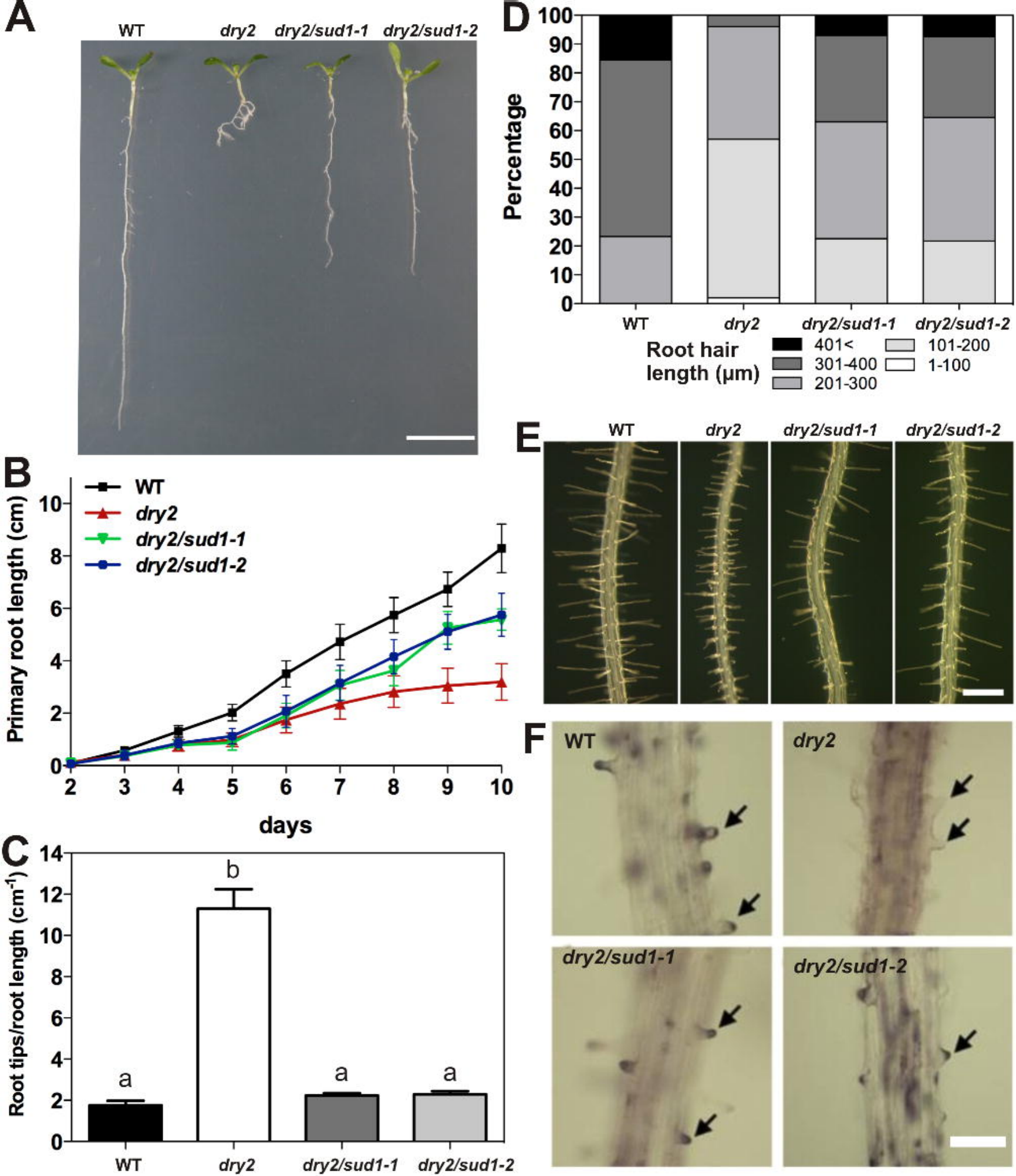
A
WT
dry2
dry2/sud1-1
dry2/sud1-2
B
WT
dry2
dry2/sud1-1
dry2/sud1-2
Primary root length (cm)
days
C
Root tips/root length (cm-1)
a
b
a
a
WT
dry2
dry2/sud1-1
dry2/sud1-2
D
Percentage
Root hair length (μm)
401<
301-400
201-300
101-200
1-100
E
F

A Phenotype of the F1 crosses with the suppressors

♀/♂	*dry2*	*dry2/sud1-1*	*dry2/sud1-2*
dry2	dry2	intermediate	intermediate
dry2/sud1-1	intermediate	WT	WT
dry2/sud1-2	intermediate	WT	WT

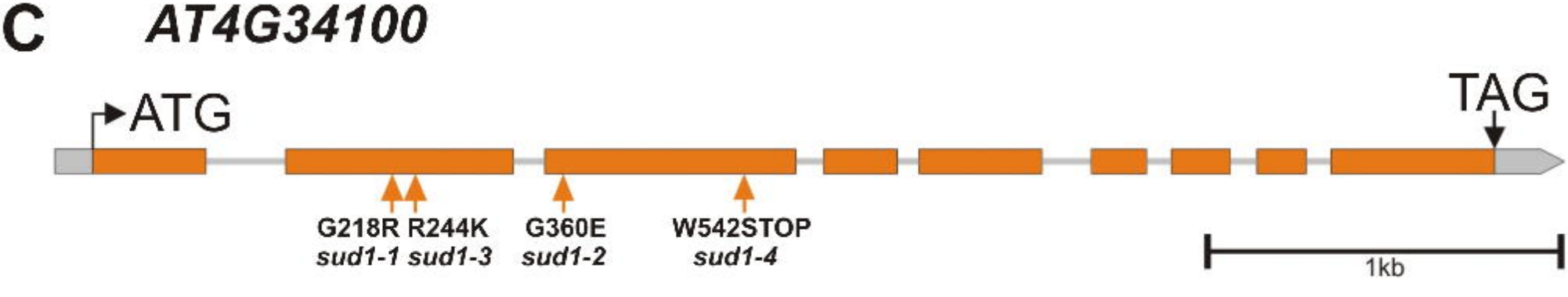

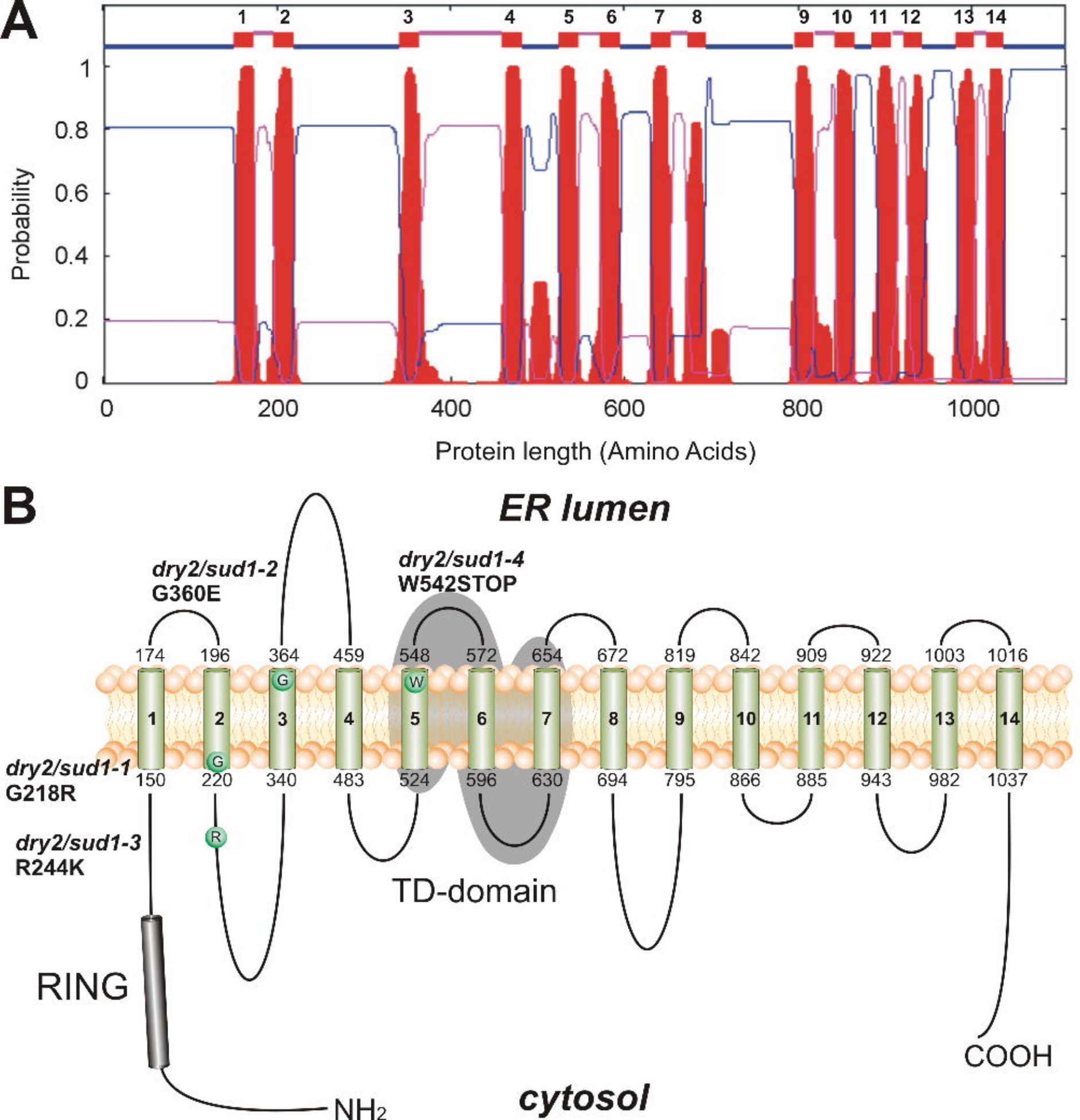
A
1 2 3 4 5 6 7 8 9 10 11 12 13 14
Probability
0
0.2
0.4
0.6
0.8
1
0
200
400
600
800
1000
Protein length (Amino Acids)
B
ER lumen
dry2/sud1-2
G360E
dry2/sud1-4
W542STOP
174 196 364 459 548 572 654 672 819 842 909 922 1003 1016
1 2 3 4 5 6 7 8 9 10 11 12 13 14
G
W
G
dry2/sud1-1
G218R
150 220 340 483 524 596 630 694 795 866 885 943 982 1037
R
dry2/sud1-3
R244K
TD-domain
RING
COOH
NH2
cytosol

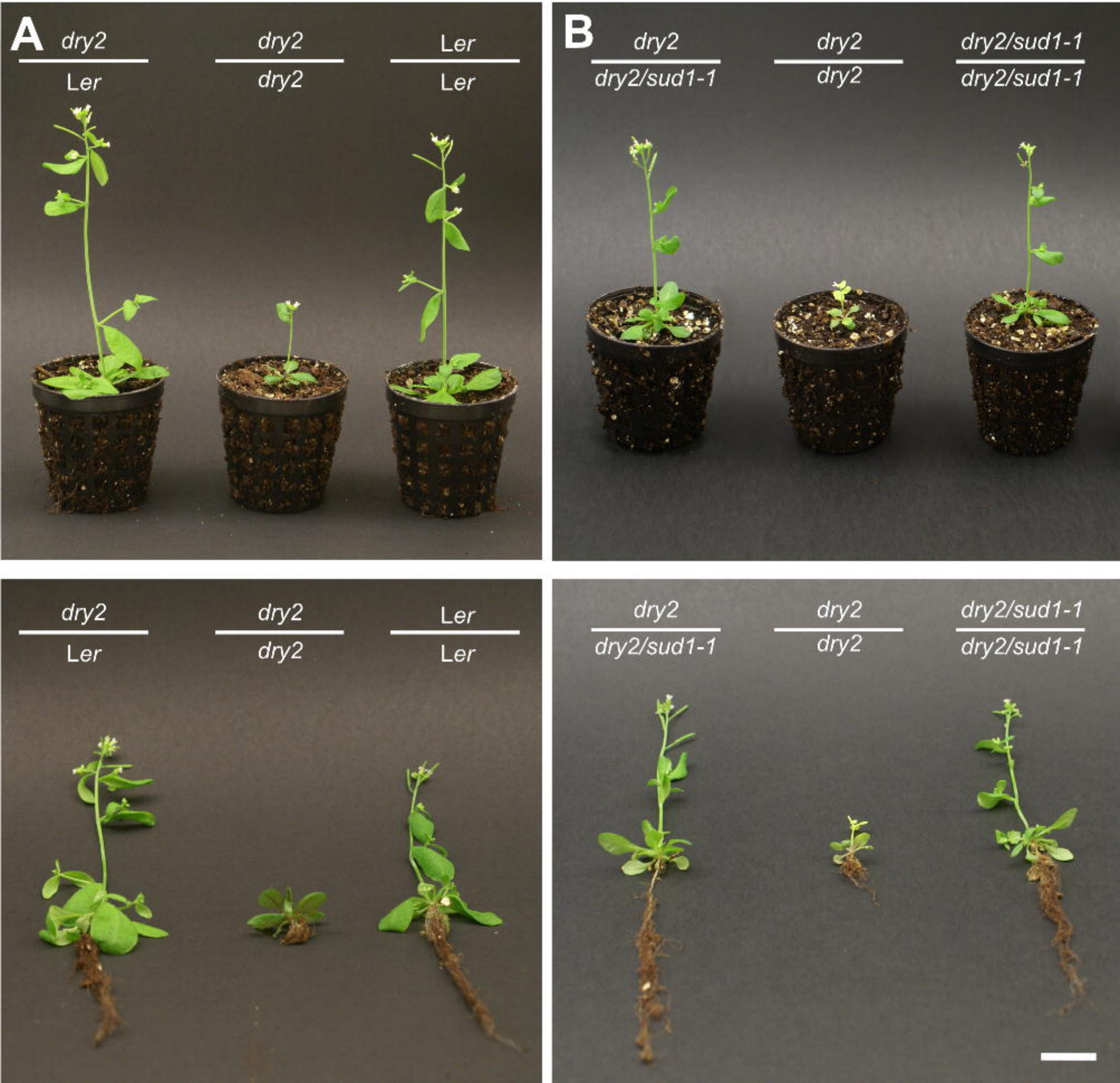
A
dry2
Ler
dry2
dry2
Ler
Ler
B
dry2
dry2/sud1-1
dry2
dry2
dry2/sud1-1
dry2/sud1-1
dry2
Ler
dry2
dry2
Ler
Ler
dry2
dry2/sud1-1
dry2
dry2
dry2/sud1-1
dry2/sud1-1

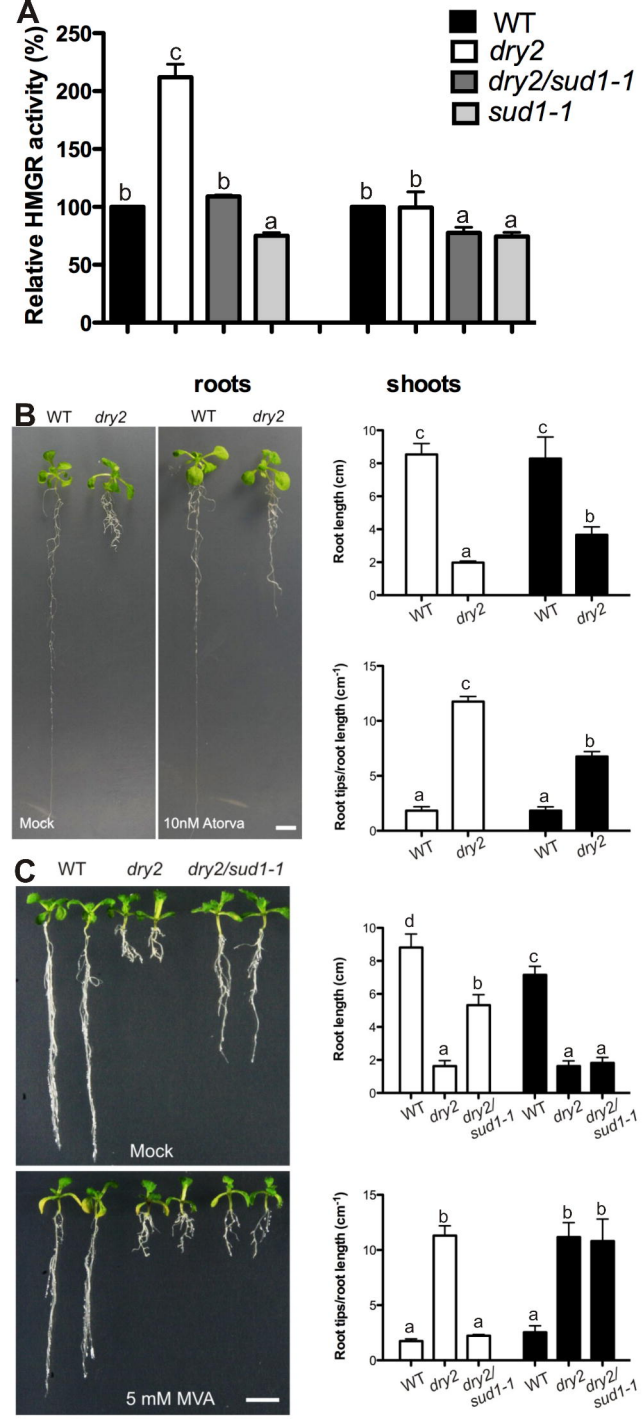
A
Relative HMGR activity (%)
250
200
150
100
50
0
WT
dry2
dry2/sud1-1
sud1-1
b
c
b
a
b
b
a
a
roots
shoots
B
WT
dry2
WT
dry2
Mock
10nM Atorva
Root length (cm)
Root tips/root length (cm-1)
C
WT
dry2
dry2/sud1-1
Mock
5 mM MVA
Root length (cm)
Root tips/root length (cm-1)

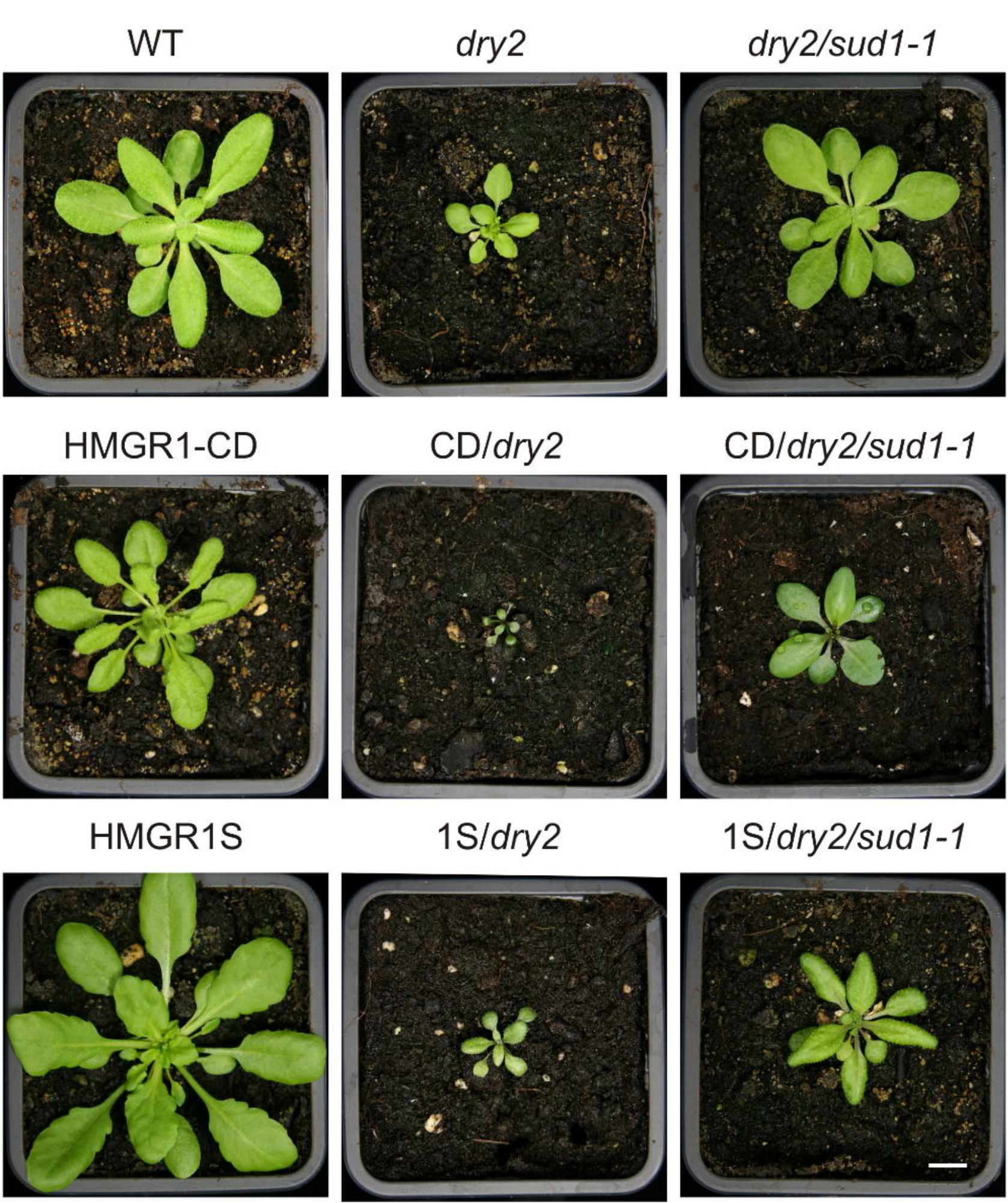
WT
dry2
dry2/sud1-1
HMGR1-CD
CD/dry2
CD/dry2/sud1-1
HMGR1S
1S/dry2
1S/dry2/sud1-1

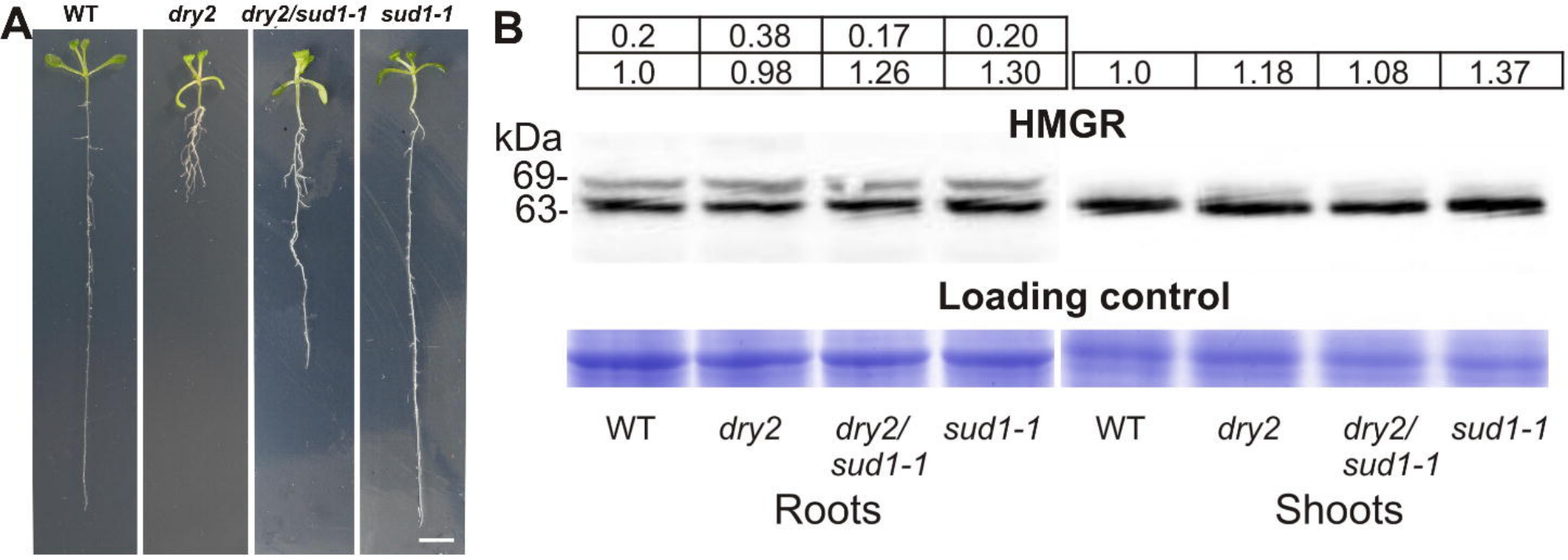
A
WT
dry2
dry2/sud1-1
sud1-1
B
0.2
0.38
0.17
0.20
1.0
0.98
1.26
1.30
1.0
1.18
1.08
1.37
HMGR
kDa
69-
63-
Loading control
WT
dry2
dry2/ sud1-1
sud1-1
WT
dry2
dry2/ sud1-1
sud1-1
Roots
Shoots


WT
dry2
M2 population

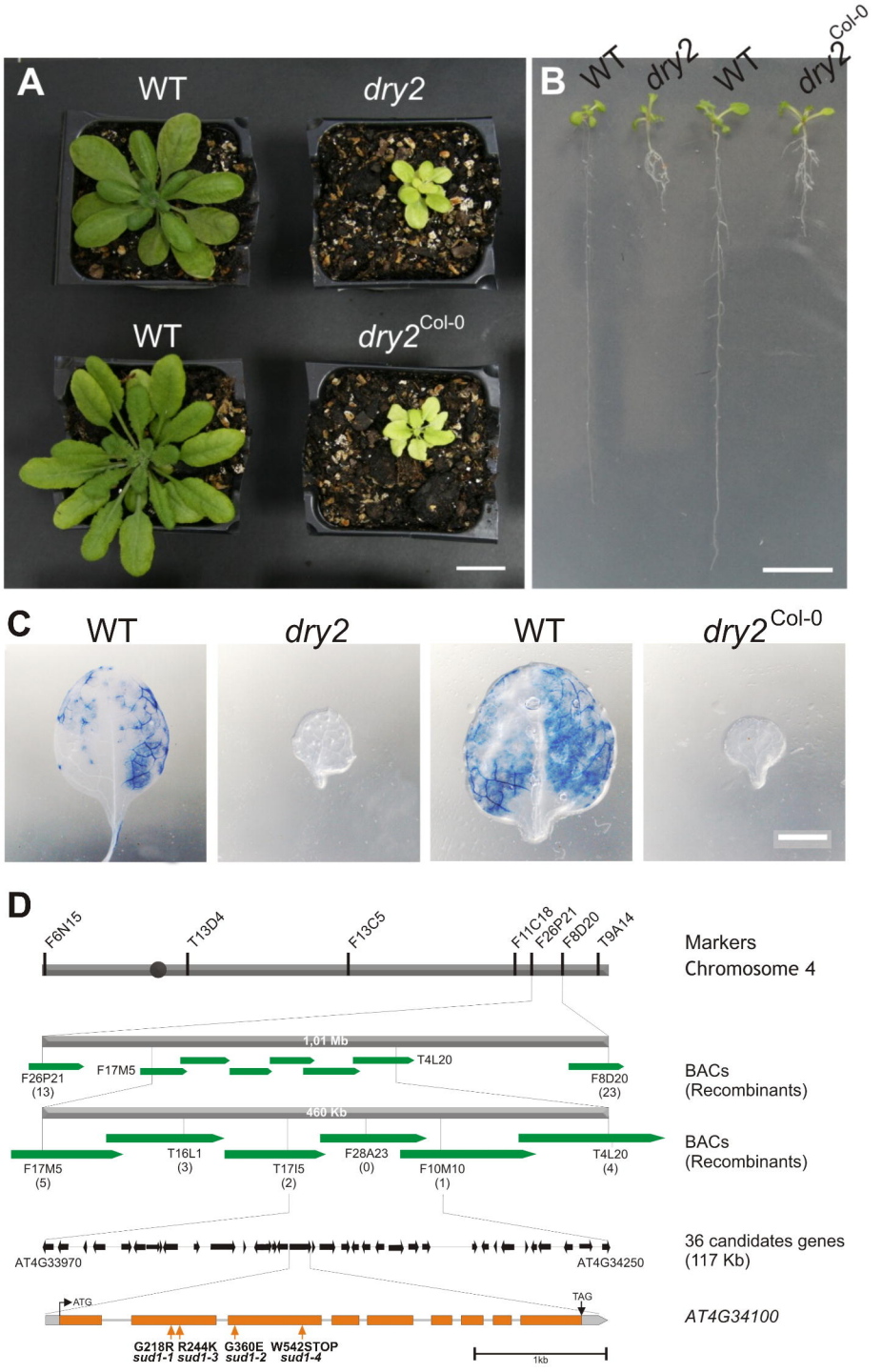
A
WT
dry2
WT
dry2Col-0
B
WT
dry2
WT
dry2Col-0
C
WT
dry2
WT
dry2Col-0
D
F6N15
T13D4
F13C5
F11C18
F26P21
F8D20
T9A14
Markers
Chromosome 4
1,01 Mb
F26P21
(13)
F17M5
T4L20
F8D20
(23)
BACs
(Recombinants)
460 Kb
F17M5
(5)
T16L1
(3)
T17I5
(2)
F28A23
(0)
F10M10
(1)
T4L20
(4)
BACs
(Recombinants)
AT4G33970
AT4G34250
36 candidates genes
(117 Kb)
ATG
TAG
G218R R244K G360E W542STOP
sud1-1 sud1-3 sud1-2 sud1-4
1kb
AT4G34100

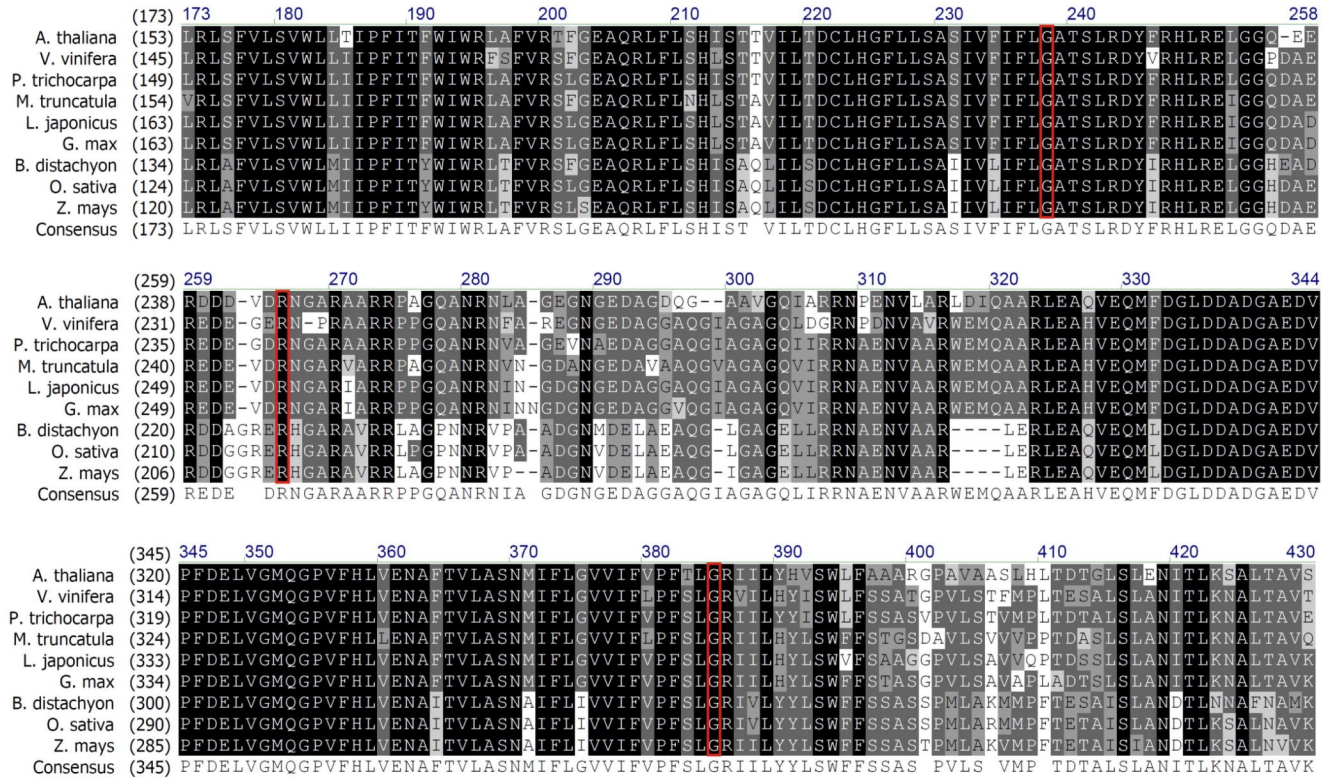
(173) 173 180 190 200 210 220 230 240 258
A. thaliana (153) LRLSFVLSVWLLTIPFITFWIWRLAFVRTFGEAQRLFLSHISTTVILTDCLHGFLLSASIVFIFLGATSLRDYFRHLRELGGQ-EE
V. vinifera (145) LRLSFVLSVWLLIIPFITFWIWRFSFVRSFGEAQRLFLSHLSTTVILTDCLHGFLLSASIVFIFLGATSLRDYVRHLRELGGPDAE
P. trichocarpa (149) LRLSFVLSVWLLIIPFITFWIWRLAFVRSLGEAQRLFLSHISTTVILTDCLHGFLLSASIVFIFLGATSLRDYFRHLRELGGQDAE
M. truncatula (154) VRLSFVLSVWLLIIPFITFWIWRLAFVRSFGEAQRLFLNHLSTAVILTDCLHGFLLSASIVFIFLGATSLRDYFRHLREIGGQDAE
L. japonicus (163) LRLSFVLSVWLLIIPFITFWIWRLAFVRSLGEAQRLFLSHLSTAVILTDCLHGFLLSASIVFIFLGATSLRDYFRHLREIGGQDAD
G. max (163) LRLSFVLSVWLLIIPFITFWIWRLAFVRSLGEAQRLFLSHLSTAVILTDCLHGFLLSASIVFIFLGATSLRDYFRHLREIGGQDAD
B. distachyon (134) LRLAFVLSVWLMIIPFITYWIWRLTFVRSFGEAQRLFLSHISAQLILSDCLHGFLLSAIVLIFLGATSLRDYIRHLRELGGHEAD
O. sativa (124) LRLAFVLSVWLMIIPFITYWIWRLTFVRSLGEAQRLFLSHISAQLILSDCLHGFLLSAIVLIFLGATSLRDYIRHLRELGGHDAE
Z. mays (120) LRLAFVLSVWLMIIPFITYWIWRLTFVRSLSEAQRLFLSHISAQLILSDCLHGFLLSAIVLIFLGATSLRDYIRHLRELGGHDAE
Consensus (173) LRLSFVLSVWLLIIPFITFWIWRLAFVRSLGEAQRLFLSHIST VILTDCLHGFLLSASIVFIFLGATSLRDYFRHLRELGGQDAE
(259) 259 270 280 290 300 310 320 330 344
A. thaliana (238) RDDD-VDRNGARAARRPAGQANRNLA-GEGNGEDAGDQG--AAVGQIARRNPENVLARLDIQAARLEAQVEQMFDGLDDADGAEDV
V. vinifera (231) REDE-GERN-PRAARRPPGQANRNFA-REGNGEDAGGAQGIAGAGQLDGRNPDNVAVRWEMQAARLEAHVEQMFDGLDDADGAEDV
P. trichocarpa (235) REDE-GDRNGARAARRPPGQANRNVA-GEVNAEDAGGAQGIAGAGQIIRRNAENVAARWEMQAARLEAHVEQMFDGLDDADGAEDV
M. truncatula (240) REDE-VDRNGARVARRPAGQANRNVN-GDANGEDAVAAQGVAGAGQVIRRNAENVAARWEMQAARLEAHVEQMFDGLDDADGAEDV
L. japonicus (249) REDE-VDRNGARIARRPPGQANRNIN-GDGNGEDAGGAQGIAGAGQVIRRNAENVAARWEMQAARLEAHVEQMFDGLDDADGAEDV
G. max (249) REDE-VDRNGARIARRPPGQANRNINNGDGNGEDAGGVQGIAGAGQVIRRNAENVAARWEMQAARLEAHVEQMFDGLDDADGAEDV
B. distachyon (220) RDDAGRERHGARAVRRLAGPNNRVPA-ADGNMDELAEAQG-LGAGELLRRNAENVAAR----LERLEAQVEQMLDGLDDADGAEDV
O. sativa (210) RDDGGRERHGARAVRRLPGPNNRVPA-ADGNVDELAEAQG-LGAGELLRRNAENVAAR----LERLEAQVEQMLDGLDDADGAEDV
Z. mays (206) RDDGGRERHGARAVRRLAGPNNRVP--ADGNVDELAEAQG-IGAGELLRRNAENVAAR----LERLEAQVEQMLDGLDDADGAEDV
Consensus (259) REDE DRNGARAARRPPGQANRNIA GDGNGEDAGGAQGIAGAGQLIRRNAENVAARWEMQAARLEAHVEQMFDGLDDADGAEDV
(345) 345 350 360 370 380 390 400 410 420 430
A. thaliana (320) PFDELVGMQGPVFHLVENAFTVLASNMIFLGVVIFVPFTLGRIILYHVSWLFAAARGPAVAASLHLTDTGLSLENITLKSALTAVS
V. vinifera (314) PFDELVGMQGPVFHLVENAFTVLASNMIFLGVVIFLPFSLGRVILHYISWLFSSATGPVLSTFMPLTESALSLANITLKNALTAVT
P. trichocarpa (319) PFDELVGMQGPVFHLVENAFTVLASNMIFLGVVIFVPFSLGRIILYYISWLFSSASVPVLSTVMPLTDTALSLANITLKNALTAVE
M. truncatula (324) PFDELVGMQGPVFHLLENAFTVLASNMIFLGVVIFLPFSLGRIILHYLSWFFSTGSDAVLSVVVPPTDASLSLANITLKNALTAVQ
L. japonicus (333) PFDELVGMQGPVFHLVENAFTVLASNMIFLGVVIFVPFSLGRIILHYLSWVFSAAGGPVLSAVVQPTDSSLSLANITLKNALTAVK
G. max (334) PFDELVGMQGPVFHLVENAFTVLASNMIFLGVVIFVPFSLGRIILHYLSWFFSTASGPVLSAVAPLADTSLSLANITLKNALTAVK
B. distachyon (300) PFDELVGMQGPVFHLVENAITVLASNAIFLIVVIFVPFSLGRIVLYYLSWFFSSASSPMLAKMMPFTESAISLANDTLNNAFNAMK
O. sativa (290) PFDELVGMQGPVFHLVENAITVLASNAIFLIVVIFVPFSLGRIVLYYLSWFFSSASSPMLARMMPFTETAISLANDTLKSALNAVK
Z. mays (285) PFDELVGMQGPVFHLVENAITVLASNAIFLIVVIFVPFSLGRIILYYLSWFFSSASTPMLAKVMPFTETAISTANDTLKSALNVVK
Consensus (345) PFDELVGMQGPVFHLVENAFTVLASNMIFLGVVIFVPFSLGRIILYYLSWFFSSAS PVLS VMP TDTALSLANITLKNALTAVK

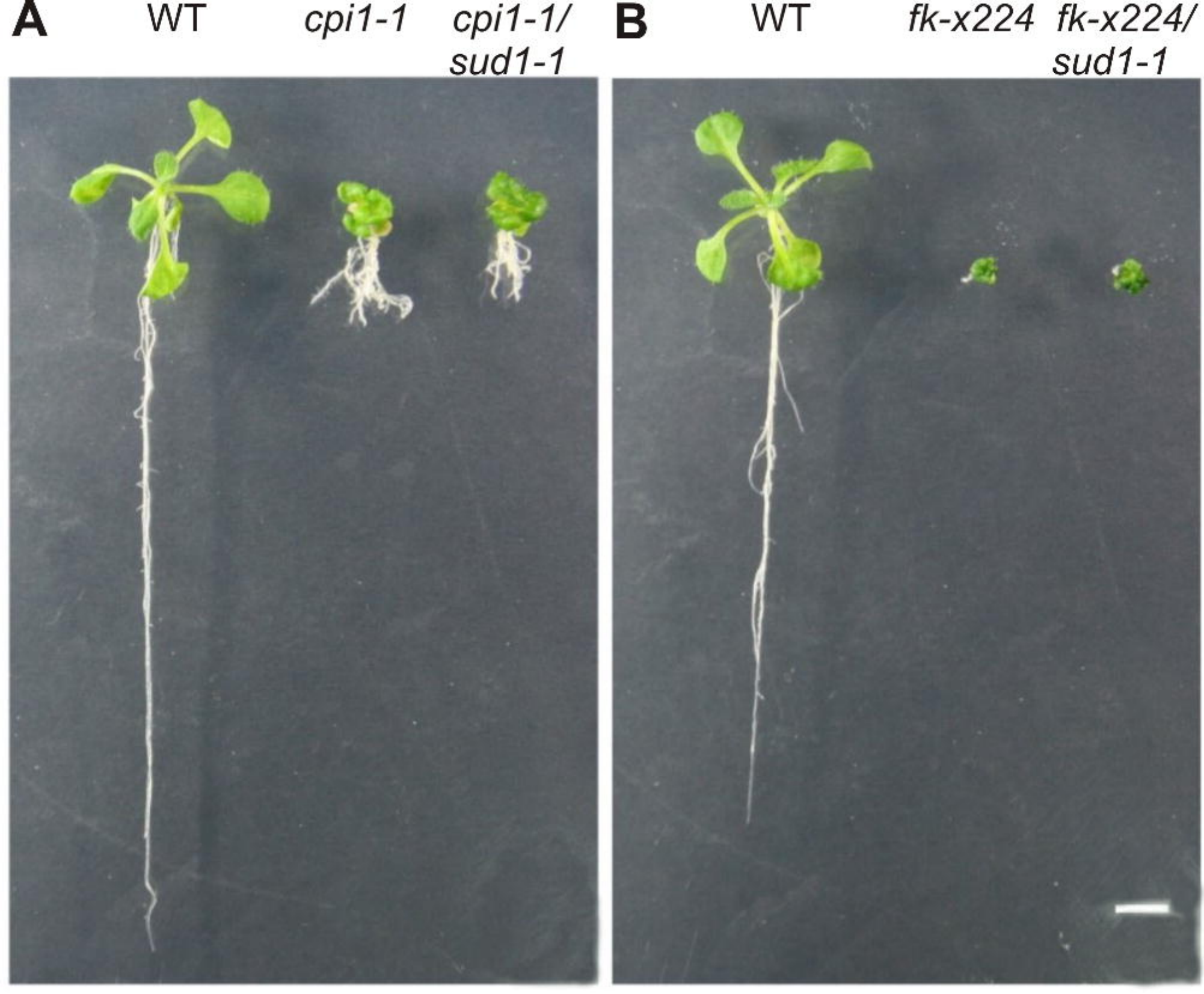
A
WT
cpi1-1
cpi1-1/
sud1-1
B
WT
fk-x224
fk-x224/
sud1-1

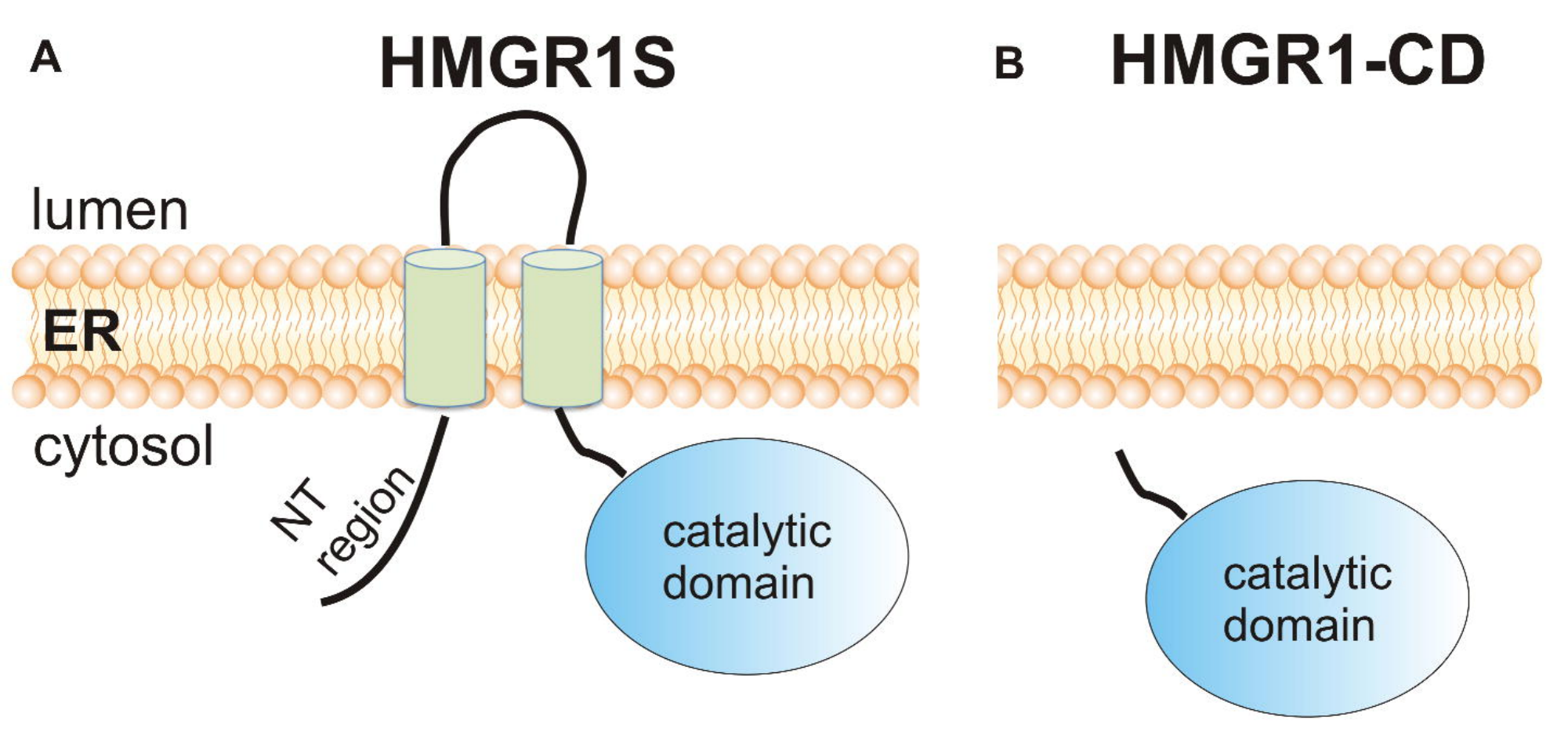
A
HMGR1S
lumen
ER
cytosol
NT region
catalytic domain
B
HMGR1-CD
catalytic domain


WT
sud1-1